



# Geographic location of St. Petersburg





# St. Petersburg

the capital of Russia since 1703 till 1918





Mariinskii theater

Pushkin

Hermitage

Pavlovsk

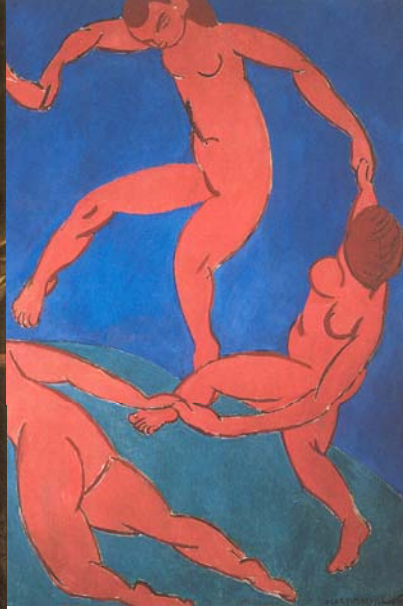
Russian Museum

Peterhof

Palaces and Squares of St. Petersburg

# Parks and Palaces of St. Petersburg Suburbs





# Treasures of Art in our Museums



# White Nights season





# Ioffe Institute of RAS

1918 — Physical-Technical Department of the State Institute of X-Rays and Radiology was founded by **Prof. M. I. Nemenov** and **A. F. Ioffe**

**Nobel Prize Winners** which works in the Ioffe Institute :  
**N. N. Semenov**, L. D. Landau, P. L. Kapitsa,  
I. E. Tamm, **Zh. I. Alferov**

**Soviet Nuclear Programme Leaders** :  
I. V. Kurchatov, A. P. Aleksandrov,  
Ya. B. Zel'dovich

Total staff - **2000**  
researchers – **1100**

Several hundred of former Ioffe researchers  
are spread around the globe





# Ioffe Institute of RAS



Division  
of Plasma Physics,  
Atomic Physics and  
Astrophysics

Division  
of Solid State  
Electronics

Division of Solid  
State Physics

Division  
of Physics  
of Dielectric and  
Semiconductors

Centre of  
Nanoheterostructure  
Physics



# Ioffe Institute of RAS



**Abraham Ioffe**  
**1918**

- ❖ **Point defect theory** (1926, Frenkel)
- ❖ **Prediction and discovery of the excitons** (Frenkel, 1932, Gross, 1951)
- ❖ **Start of Russian Nuclear project** (Kurchatov, 1940s)
- ❖ **Prediction and first experimental confirmation of semiconductor properties of III-V compounds (InSb)** (1950, Goryunova, Regel)
- ❖ **Studies of excitonic properties of bulk II-VI materials** (in 60th– 80th, Zakharchenya, Kapliansky, Permogorov et al.)
- ❖ **Discovery of semiconductor heterostructures** (since 1967, Alferov et al. – Nobel Prize, 2000)
- ❖ **Theory of resonance tunneling in superlattices, idea of quantum cascade laser** (1971, Kazarionov, Suris)
- ❖ **Idea of spin injection, theory of spin polarization and first experiments on optical detection of spin polarization** (1976 and later, Aronov, Pikus, Zakharchenya et al.)
- ❖ **Dyakonov-Perel spin relaxation mechanism by** (1978, Dyakonov, Perel )
- ❖ **Discovery of semiconductor quantum dots – II-VI in glass** (1982, Ekimov, Efros)
- ❖ **Lowest threshold AlGaAs QW SCH laser diode ( $40 \text{ A/cm}^2$ ) with GRIN SL waveguide** (Alferov, Ivanov, Ledentsov, Ustinov, Kop'ev, Meltser, 1988)
- ❖ **First AlGaAs laser diode with InAs QD** (Alferov and co-workers, 1994)
- ❖ **Recent works on MBE technology and studies of II-VI wide gap nanostructures for optoelectronics and spintronics** (Ivanov, Toropov, Shubina et al., 90-s)



# Quantum-size Heterostructure Lab



**MBE growth & processing**

**Total 24**

**Optical & Electrical Studies**

8	Senior Researchers and Researchers	5
3	PhD students	2
3	undergraduate students	1
1	manager, technician	1



# Group Activity Scope

**Main goal:** Molecular beam epitaxy and fundamental studies of semiconductor heterostructures (with quantum wells, quantum dots and superlattices) based on

- narrow gap III-V compounds - (Al,Ga,In)(As,Sb) - for mid-IR optoelectronics and HEMTs (**MBE setup Riber 32P, France**);
- wide gap II-VI compounds - (Zn,Cd,Mg)(S,Se,Te) and ZnO - for visible (blue-green) and UV spectral range optoelectronics, including lasers with electron beam and optical pumping, as well as spintronic studies of diluted magnetic semiconductor heterostructures (**double chamber III-V/II-VI MBE setup, Semiteq, Russia**);
- hybrid III-V/II-VI structures with a heterovalent interface in the active region for mid-IR applications, solar cells, and spintronics (**double chamber III-V/II-VI MBE setup, Semiteq, Russia**);
- **III-nitrides - (Ga,In,Al)N** - for optoelectronic applications in visible (green-red) and **deep UV spectral ranges** as well as fundamental studies of In-riched compounds and metal-semiconductor composite nanostructures (**PA MBE setup Riber Compact 21T, France**).

## Projects

Russian Foundation for Basic Research (basic & applied research) – 12 (1 with PKU)  
Presidium of RAS, Physical Sciences Department of RAS – 5  
Russian Agency for Science and Innovations – 2  
International contracts (OSRAM, Germany; ETRI, Korea; KACST, Saudi Arabia) - 3  
Marie Curie training network on Spinoptronics (FP7) – 1  
Russian Ministry on Industry and Trade, Ministry of Defence - 2



# Plasma-assisted molecular beam epitaxy of Al(Ga)N layers and quantum well structures on c-Al<sub>2</sub>O<sub>3</sub> for mid-UV emitters and solar-blind photodiodes

**S.V. Ivanov**



## Acknowledgments

***V.N. Jmerik, D.V. Nechaev, T.A. Komissarova,  
E.A. Shevchenko, A.A. Toropov, A. A. Sitnikova, V.V. Ratnikov,  
M.A. Yagovkina***

Ioffe Physical-Technical Institute of RAS, Polytekhnicheskaya 26, St. Petersburg 194021, Russia



***E.V. Lutsenko, N.V. Rzhetskii, G.P. Yablonskii***

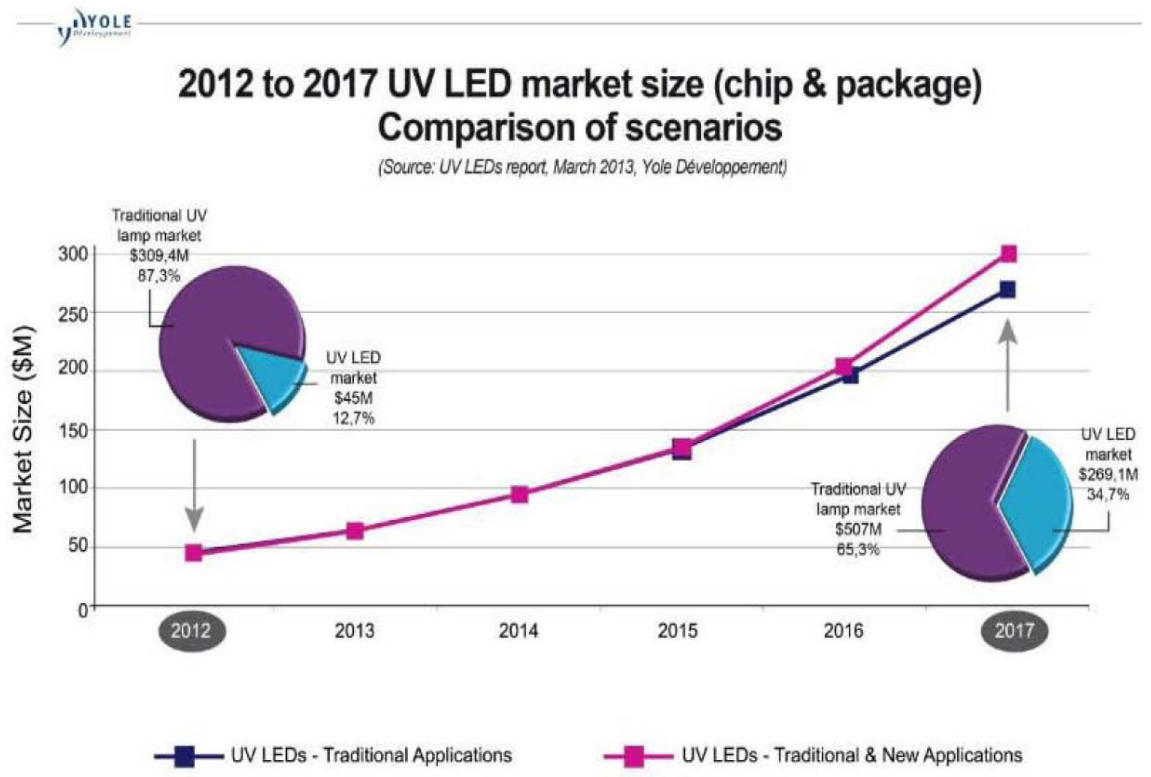
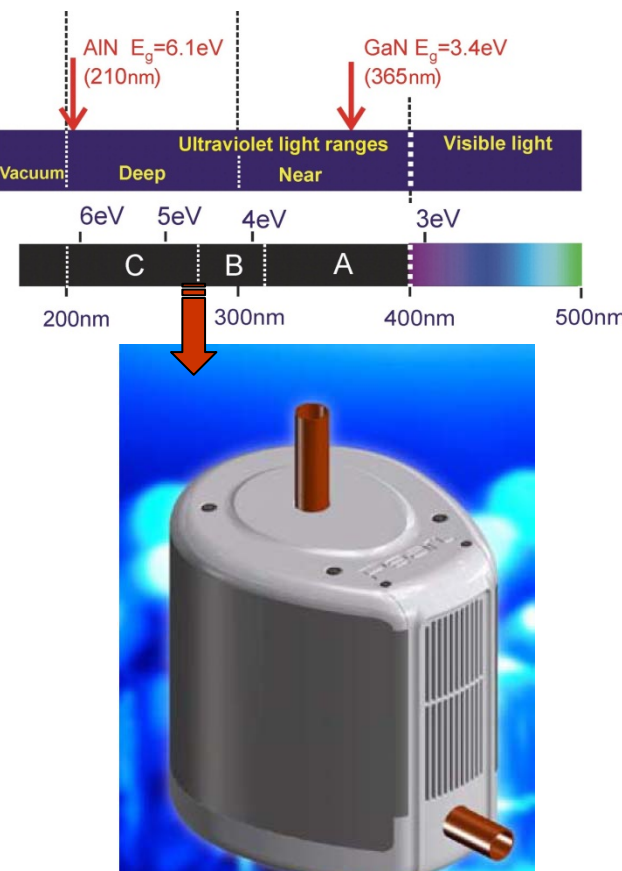
Stepanov Institute of Physics of NAS Belarus, Independence Ave. 68, Minsk 220072, Belarus



# Outline

- Applications of UV-optoelectronics and state-of-the-art of AlGaN-based UV LED and laser structures obtained by both MOVPE and PA MBE
- PA MBE growth and surface morphology control of III-Nitrides
  - Al-rich growth of thick AlN/c-Al<sub>2</sub>O<sub>3</sub> buffer layers
  - Growth kinetics of AlGaN layers (2D-3D transition)
- Dislocation control and filtering in AlGaN/AlN/c-Al<sub>2</sub>O<sub>3</sub> heterostructures
- Sub-monolayer Digital Alloying growth of Al<sub>x</sub>Ga<sub>1-x</sub>N/Al<sub>y</sub>Ga<sub>1-y</sub>N QWs
- Strain engineering in AlGaN QW heterostructures to prevent TE/TM switching of photoluminescence polarization
- Low-threshold optically pumped QW laser structures in the 258-303 nm range
- LEDs and solar-blind p-i-n photodiodes
- Conclusions

# Market and main applications of UV-optoelectronics



## Main applications of UV-lasers

UV-spectroscopy

Biomedical applications

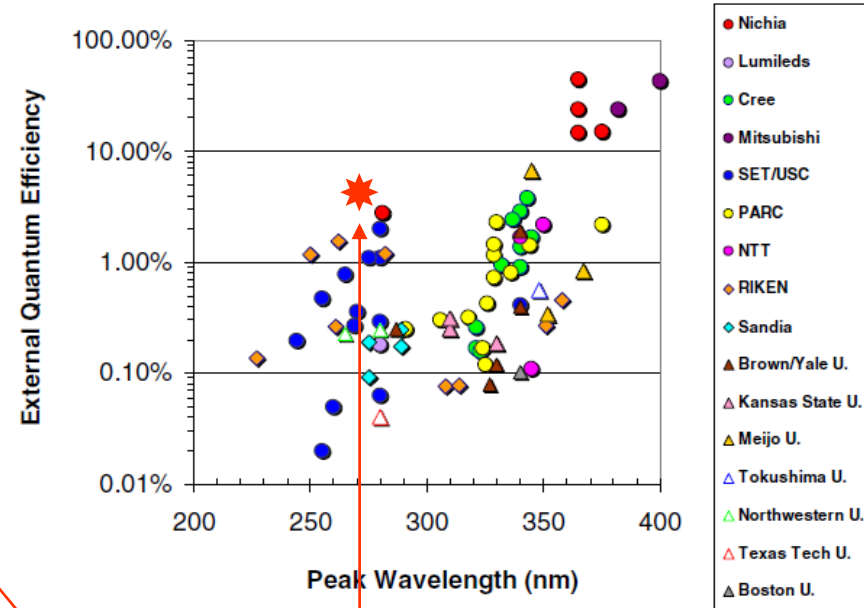
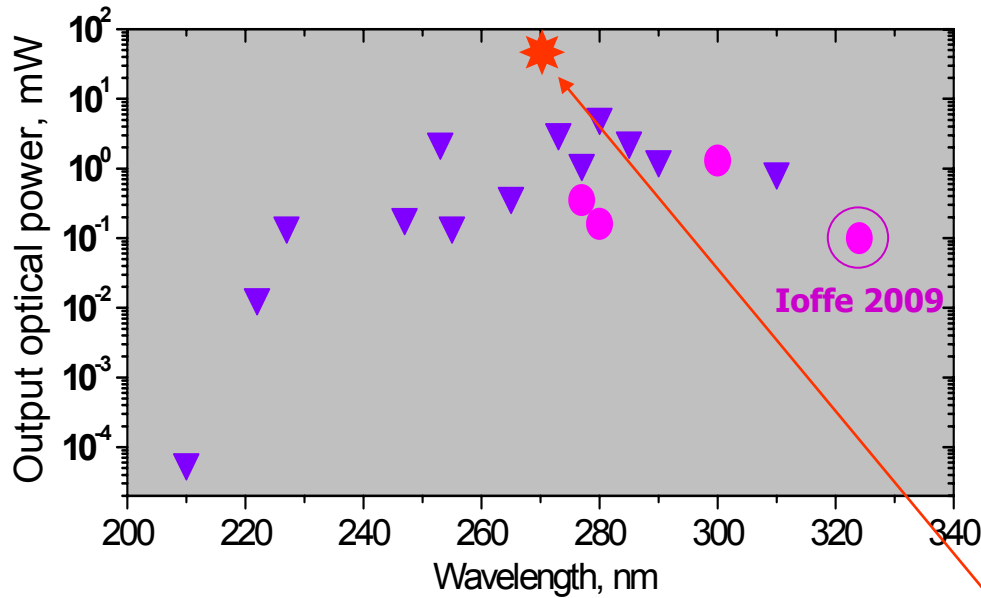
Biomedical Optics EXPRESS

Military & Security systems

UV covert communications



# State of art of UV-LEDs (2013)



M.Kneissl et al., *Semicond. Sci.Technol.* 26 (2011) 014036

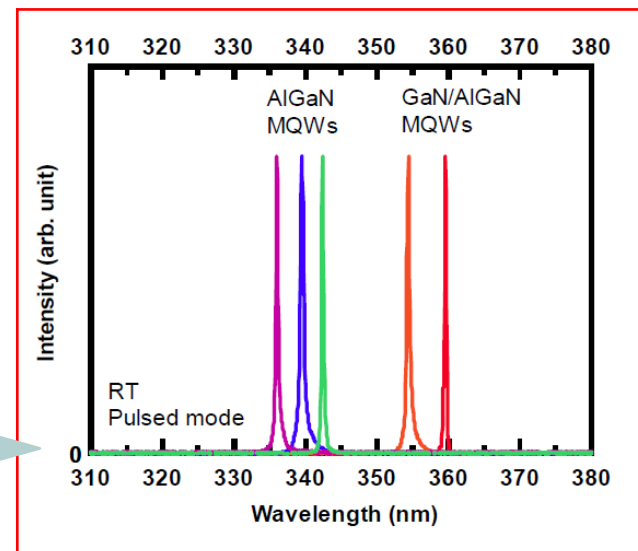
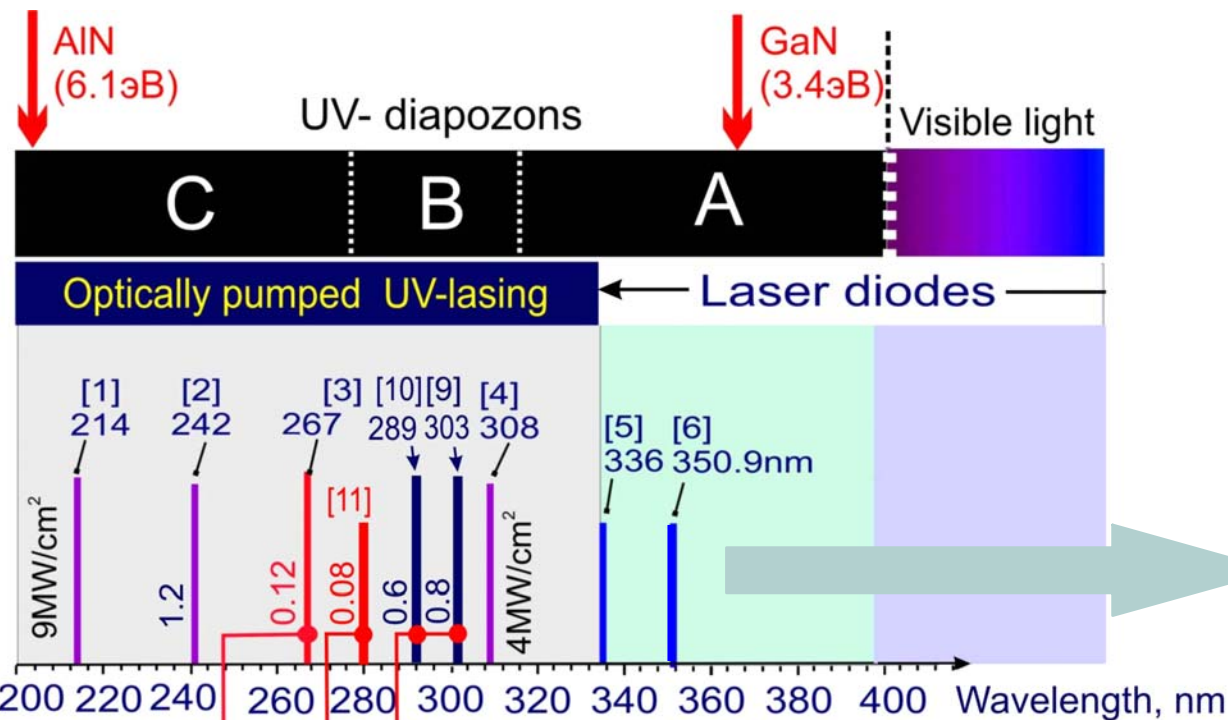
**MOCVD** ▼

**MBE** ●

**Crystal IS, Inc. & US ARL**  
 Pseudomorphic single-chip UV LED  
 on bulk AlN substrate:  
 $\lambda = 271\text{nm}$ ,  $P_{\text{out}} = 60\text{mW CW}$ ,  
 EQE = 4.9%, WPE = 2.5%

*Grandusky et al., APEX 6, 032101 (2013)*

# State-of-the-art of UV-lasers (2013)



HAMAMATSU Global

Optically pumped lasing (PA MBE):

[9] Jmerik et al. APL **96**, 141112 (2010)

[10] —//—//— PSS A, **210**, 439 (2013)

Optically pumped lasing (MOCVD):

[1] Shatalov et al., JJAP, **45**, L1286(2006).

[2] Takano et al., APL, **84**, 3567 (2004).

[3] Wunderer et al., APE, **4**, 092101, (2011).

[4] Kneisslet et al., JAP, **101**, 123103 (2007).

[11] Xie et al., APL **102**, 171102 (2013).

HexaTech, Inc., North.Carolina State Univ.,  
Army Res.Lab.

OP Lasing at 280.8 nm and with  $P_{th}=84\text{kW/cm}^2$   
on bulk AlN substrate

AlGaN-based Laser Diodes (MOCVD):

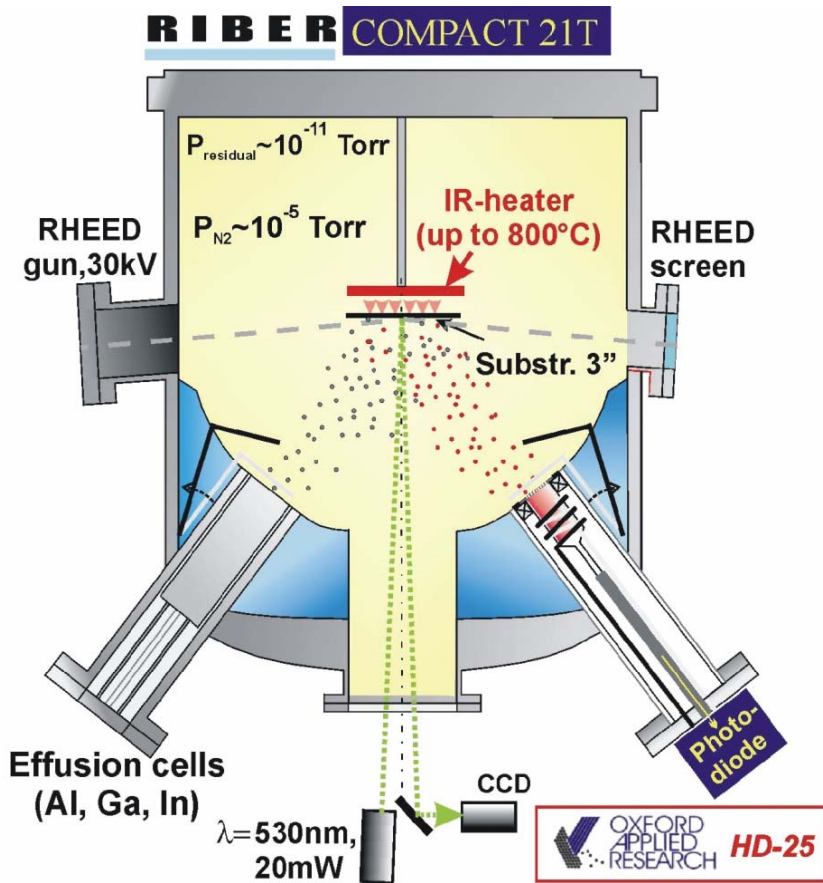
[5] Yoshida et al., APL, **93**, 241106 (2008).



# Outline

- Applications of UV-optoelectronics and state-of-the-art of AlGaN-based UV LED and laser structures obtained by both MOVPE and PA MBE
- PA MBE growth and surface morphology control of III-Nitrides
  - Al-rich growth of thick AlN/c-Al<sub>2</sub>O<sub>3</sub> buffer layers
  - Growth kinetics of AlGaN layers (2D-3D transition)
- Dislocation control and filtering in AlGaN/AlN/c-Al<sub>2</sub>O<sub>3</sub> heterostructures
- Sub-monolayer Digital Alloying growth of Al<sub>x</sub>Ga<sub>1-x</sub>N/Al<sub>y</sub>Ga<sub>1-y</sub>N QWs
- Strain engineering in AlGaN QW heterostructures to prevent TE/TM switching of photoluminescence polarization
- Low-threshold optically pumped QW laser structures in the 258-303 nm range
- LEDs and solar-blind p-i-n photodiodes
- Conclusions

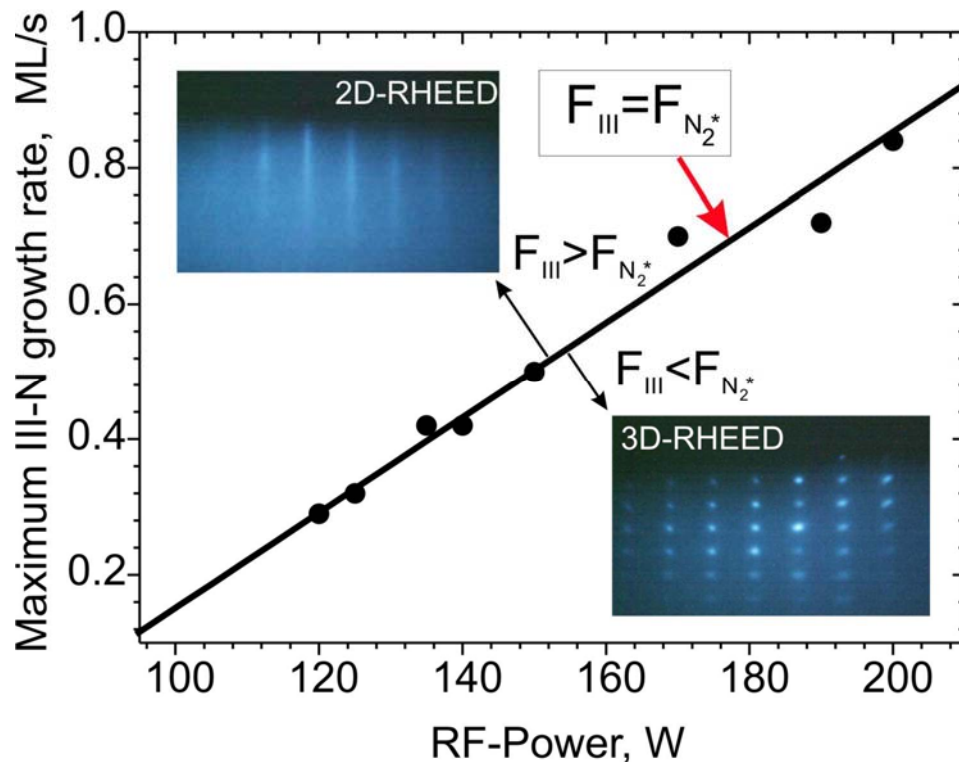
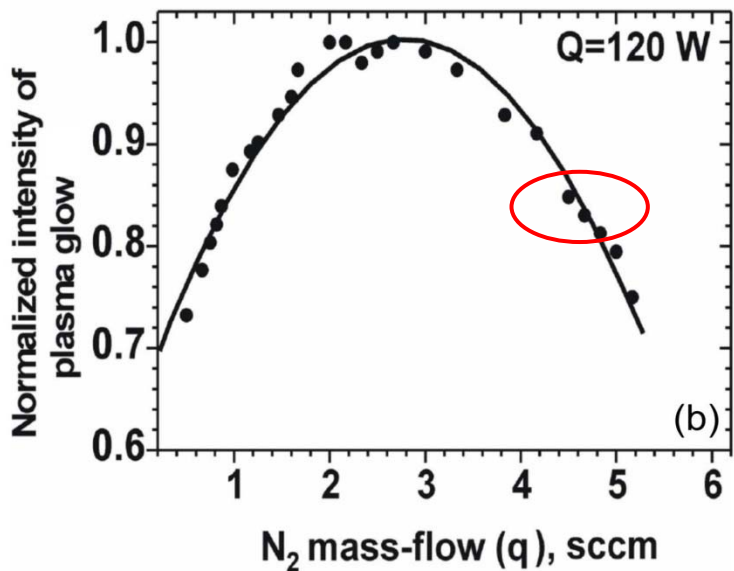
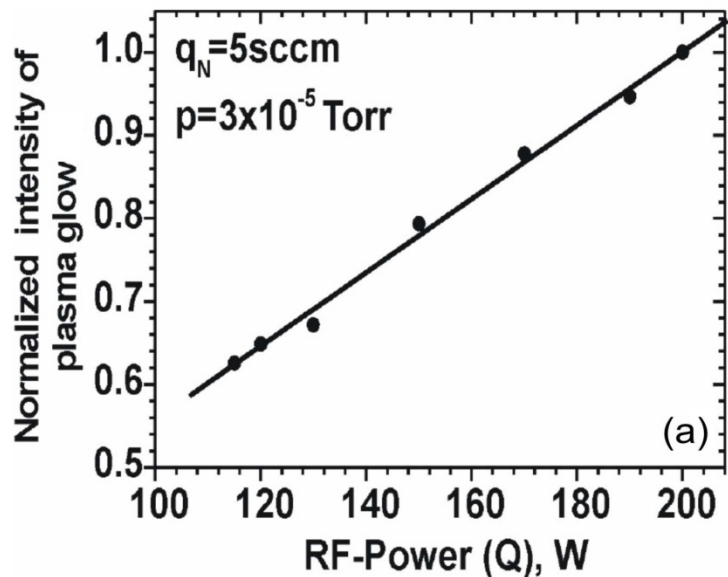
# Peculiarities & Advantages of Plasma-Assisted MBE of AlGaIn



- High vacuum growth conditions
  - *No parasitic gas-phase reactions (Al+NH<sub>3</sub>)*
- Hydrogen- and carbon-free growth environment
  - *Easy Mg doping without post-growth treatment*
- Rapid change of growth atom fluxes
- Low growth temperature (700-800°C)
  - + *Sharp interfaces with atomic resolution*
  - *Complexity of the 2D step-flow growth*
- Growth under different stoichiometric conditions:
  - nitrogen-rich (III/N < 1) → 3D growth*
  - metal-rich (III/N ≥ 1) → 2D growth*
- Variable polarity growth:
  - Ga-polar and N-polar depending on growth nucleation



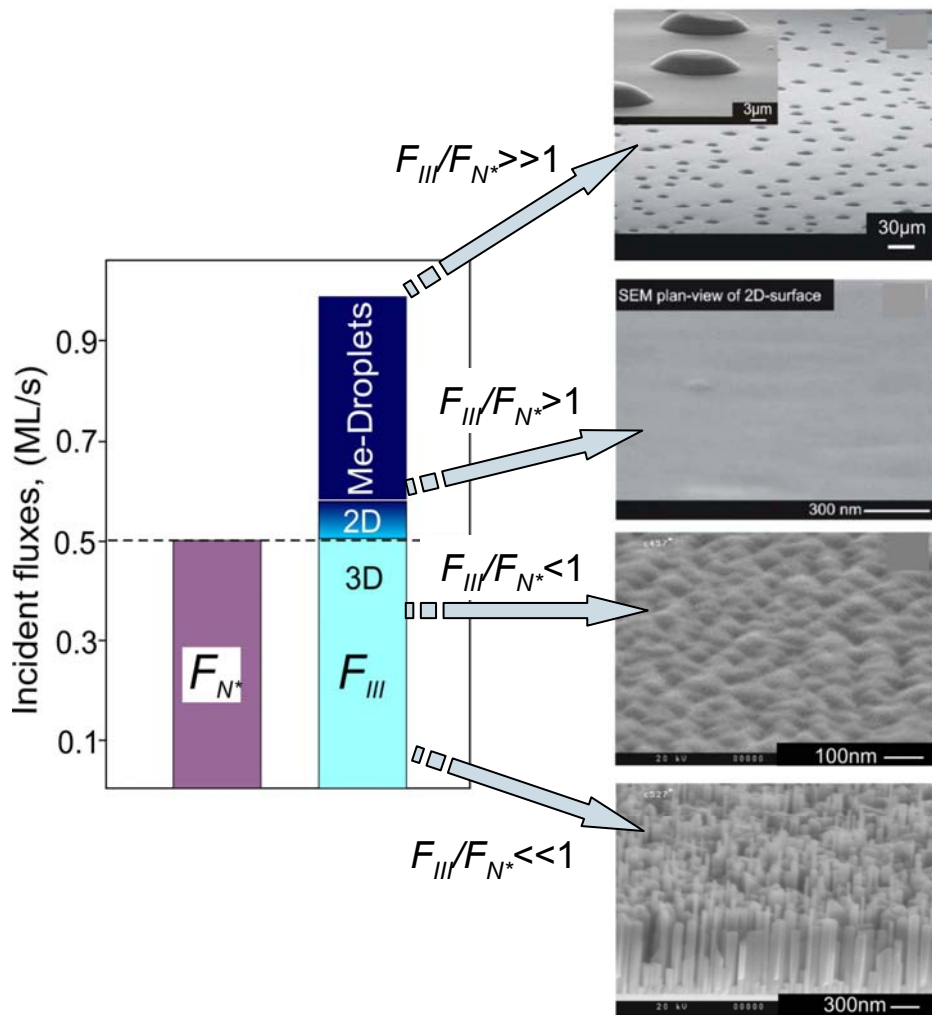
# Linear control of plasma-activated nitrogen flux



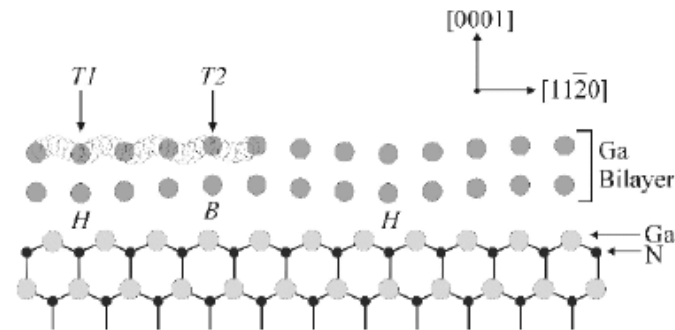
Jmerik et al., *Techn. Phys. Lett.* 33,333 (2007)



# Stoichiometrical conditions in PA MBE of III-nitrides

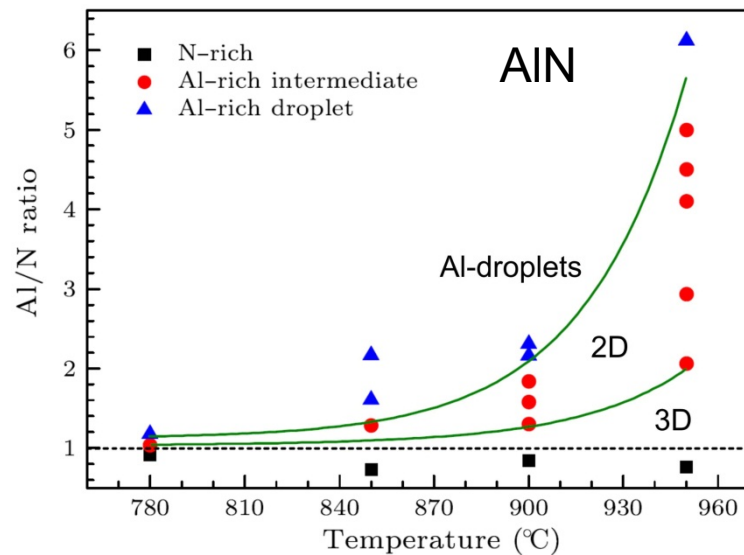


## Ga-rich PA MBE of GaN



*Heying et al., J. Appl. Phys. 88, (2000), 4.*

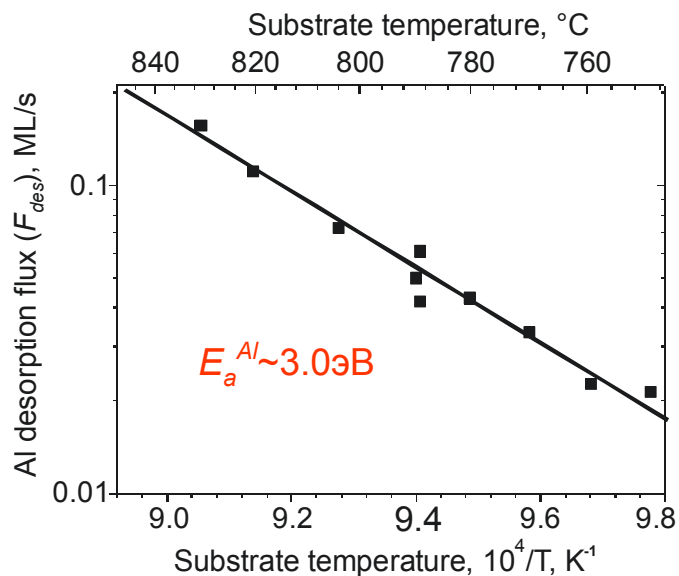
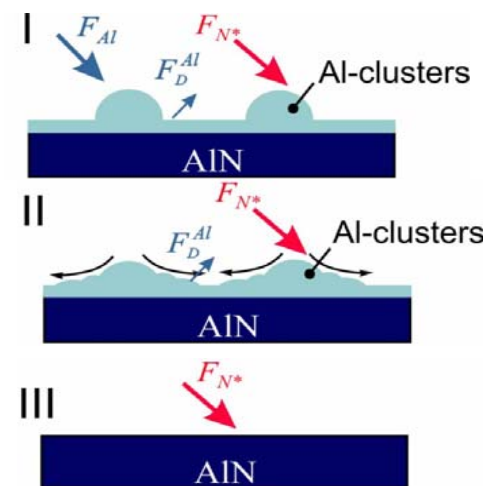
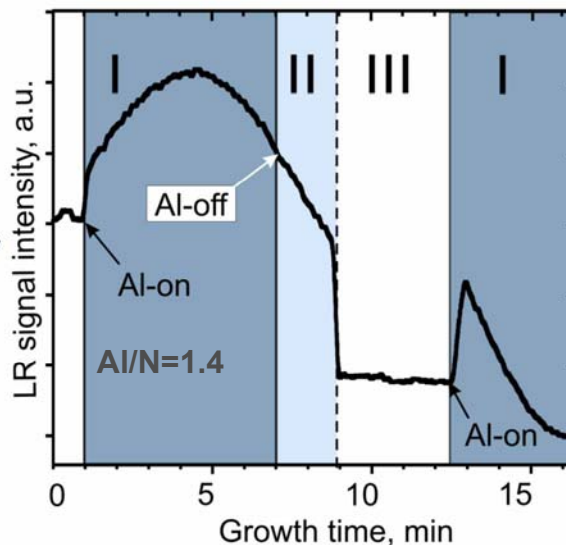
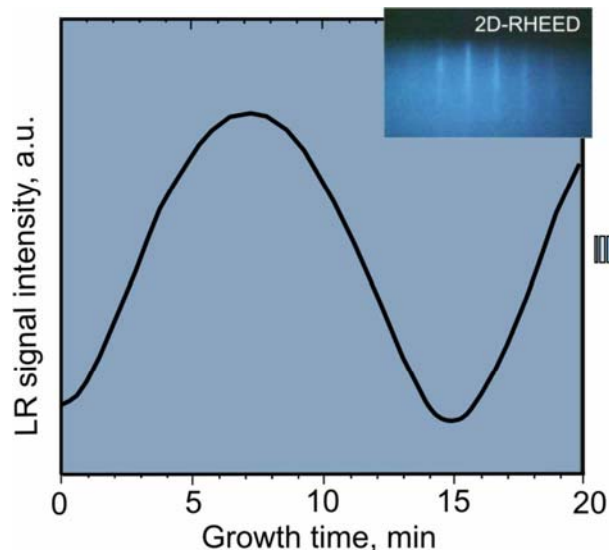
*Northrup et al., Phys.Rev.B, 61, (2000), 9932.*



*Pan et al., Chin.Phys.Lett., 28, (2011), 068102.*



# Al-rich growth of thick AlN layers with periodically supplied Al-flux and continuous N-flux



$$F_D^{Al}(T_S) = \frac{F_{Al} \cdot t_I}{t_I + t_{II}(T_S)} - F_{N^*}$$



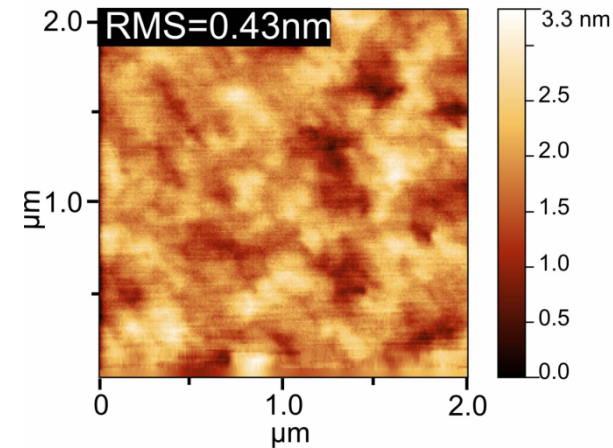
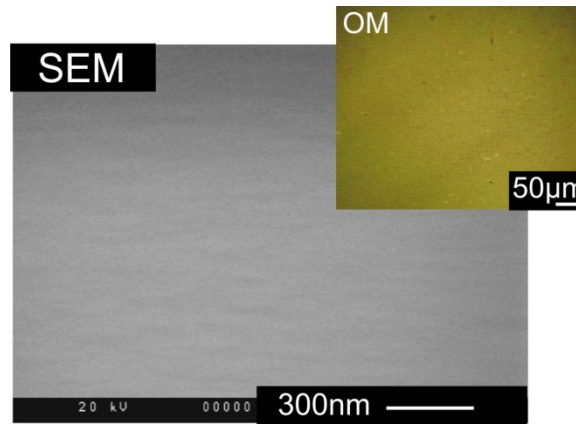
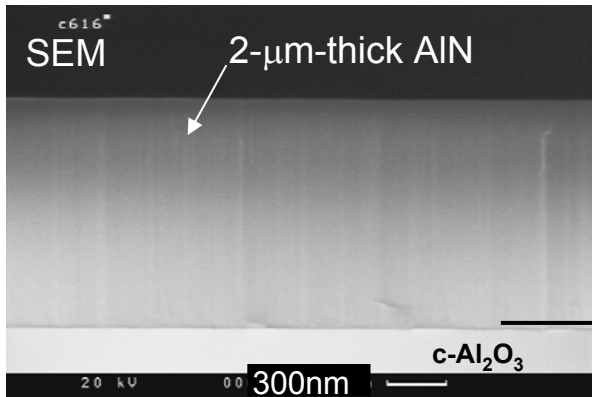
$$F_D^{Al} = A \cdot \exp\left(-\frac{E_a^{Al}}{kT_S}\right)$$

Jmerik et al., J. Cryst. Growth 354, 188 (2012)



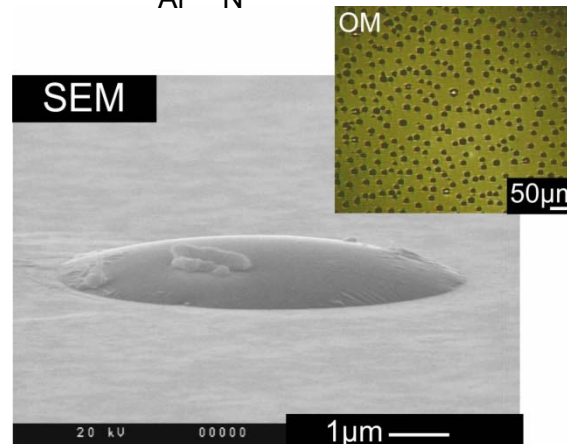
# 2- $\mu\text{m}$ -thick AlN layers with atomically smooth and droplet-free surface

Pulsed Al-supplying mode:  $T_S=730^\circ\text{C}$   $F_{\text{Al}}/F_{\text{N}}=1.4$   
 $t_I=3\text{min}$ ;  $t_{II}=45\text{s}$ ;  $t_{III}=45\text{s}$



Continuous Al-supplying mode:  $T_S=730^\circ\text{C}$   $F_{\text{Al}}/F_{\text{N}}=1.4$

Al droplets  $n\sim 10^5\text{ cm}^{-2}$



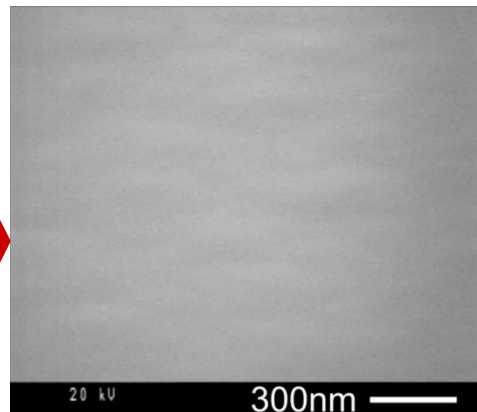


# Polarities of $\text{Al}_x\text{Ga}_{1-x}\text{N}$ ( $x=0-1$ ) layers grown by PA MBE

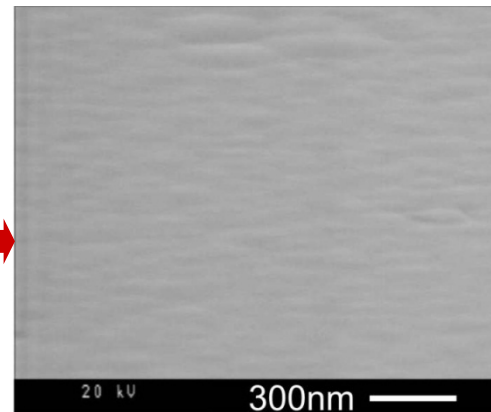
## III-polar $\text{AlGaN}(0001)$

Buffer layer/substrate	Al-content
c- $\text{Al}_2\text{O}_3$	$0.2 < x < 1$
$3\mu\text{m-GaN}(0001)$ -MOCVD	$0 < x < 1$
$300\text{nm-AlN}(0001)$ -PA MBE	$0 < x < 1$

SEM images of the  $\text{AlGaN}$  surfaces after growth

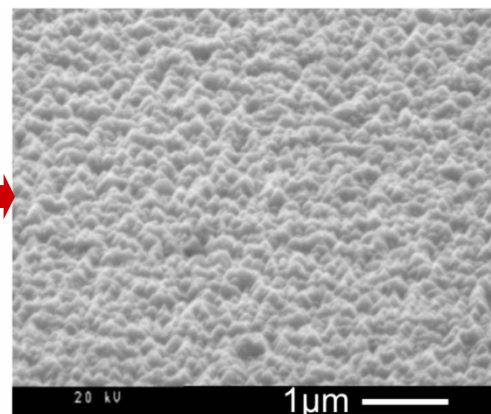
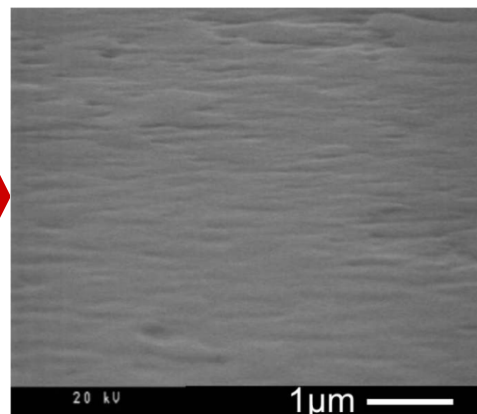


After 10-minutes etching in 0.2M KOH at 300K



## N-polar $\text{AlGaN}(000\bar{1})$

Buffer layer/substrate	Al-content
c- $\text{Al}_2\text{O}_3$	$0 < x < 0.2$
$500\text{nm-GaN}(000\bar{1})$ -PA MBE	$0 < x < 1$



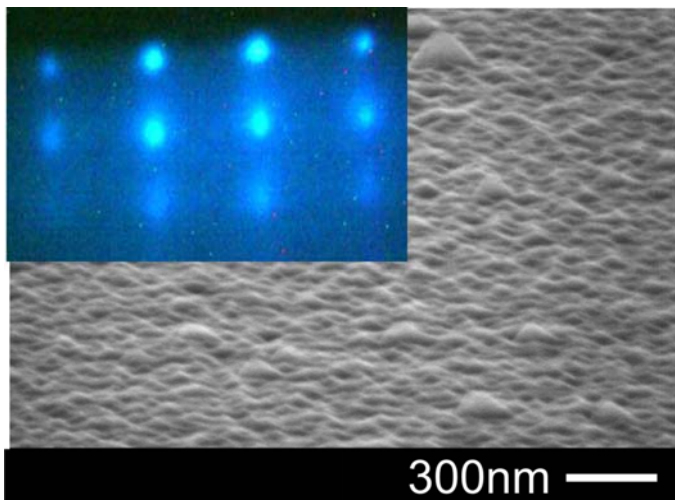
Both polarities of  $\text{Al}_x\text{Ga}_{1-x}\text{N}$  ( $0 < x < 1$ ) can be grown by PA MBE

Mizerov et al., *Semiconductors*, 43, 1096 (2009)

Peking University, May 15, 2014



# AlGaN layers with different morphologies and Al-content grown at both N- and Ga-rich conditions



## N-rich $\text{Al}_x\text{Ga}_{1-x}\text{N}$

$$F_{\text{III}}/F_{\text{N}}=0.9$$

$$T_{\text{S}}=700^{\circ}\text{C}$$

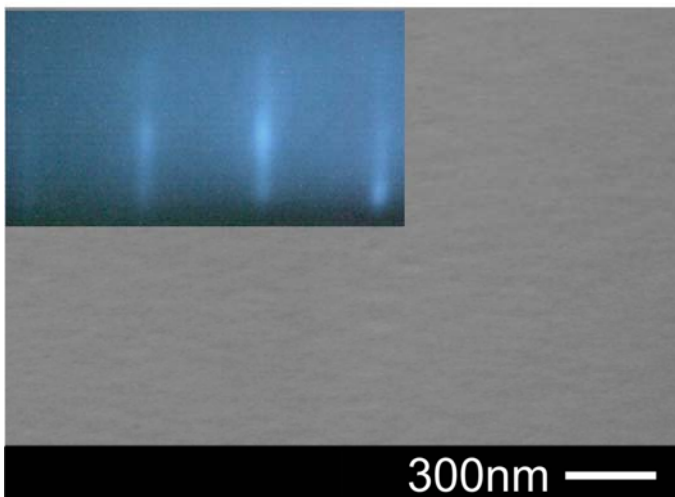
$$F_{\text{N}}=0.5\text{ML/s}$$

$$F_{\text{Al}}/F_{\text{N}}=0.7 \neq x$$

### **x depends on**

- Substrate temperature
- Stress in heterostructures
- Growth rate

*Mizerov et al., J. Cryst. Growth 323, 686 (2011).*



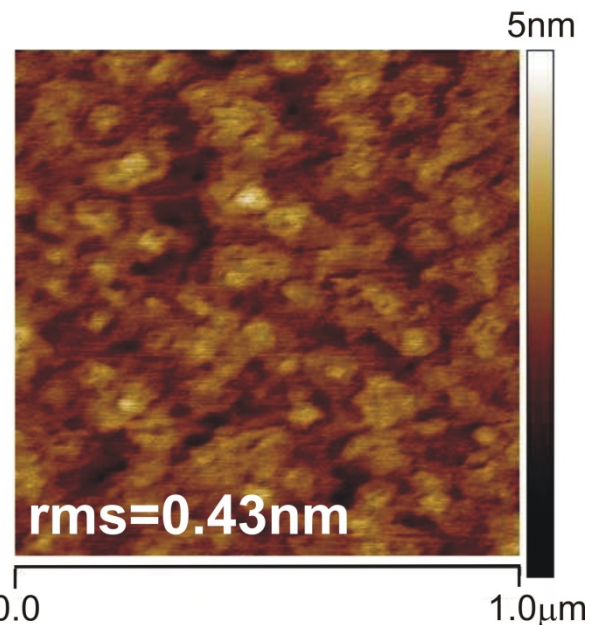
## Ga-rich $\text{Al}_{0.7}\text{Ga}_{0.3}\text{N}$

$$F_{\text{III}}/F_{\text{N}}=1.8$$

$$T_{\text{S}}=700^{\circ}\text{C}$$

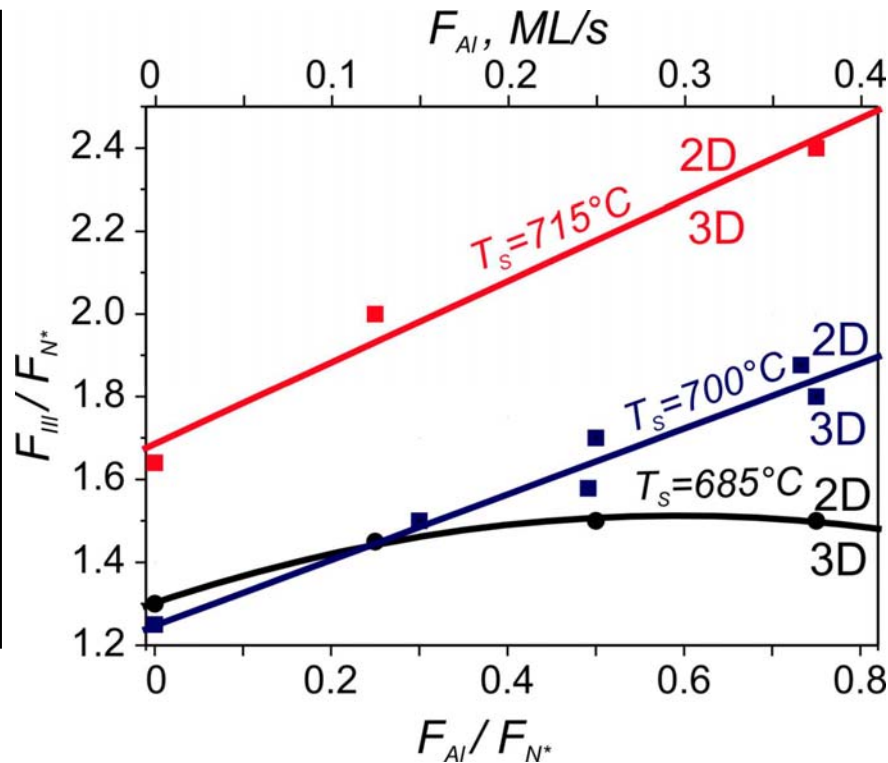
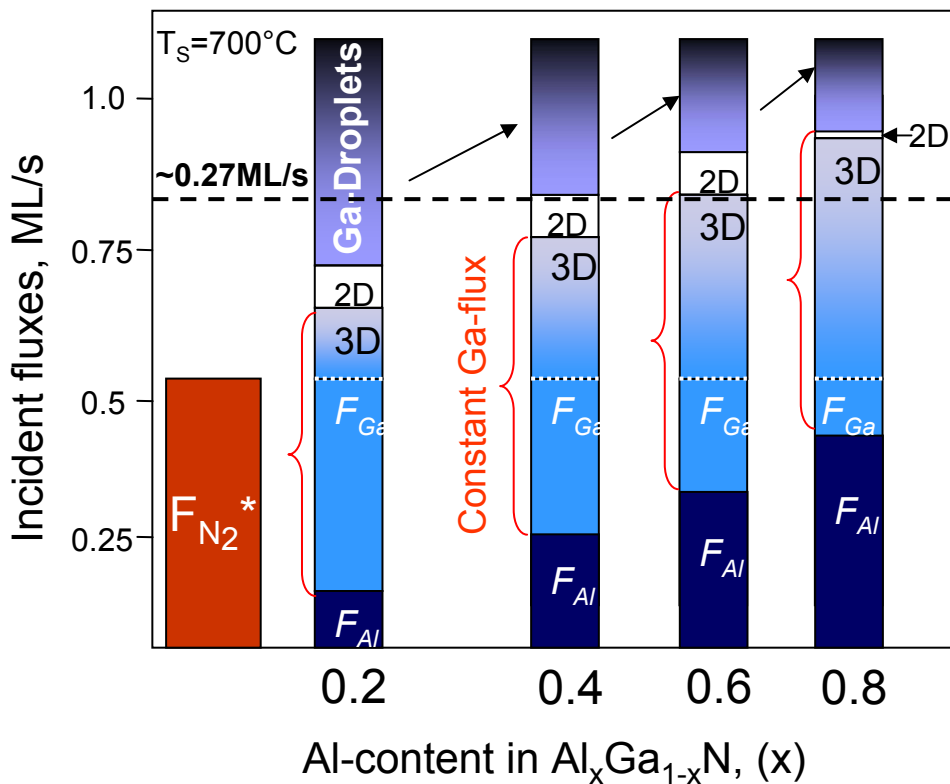
$$F_{\text{N}}=v_{\text{g}}=0.5\text{ML/s}$$

$$F_{\text{Al}}/F_{\text{N}}=x=0.7$$





# 3D-2D phase diagram of PA MBE growth of $\text{Al}_x\text{Ga}_{1-x}\text{N}$ ( $x=0-0.8$ ) layers in Ga-rich conditions



$x = F_{\text{Al}}/F_{\text{N}}$   
 $(x=0.1-1)$  at  $F_{\text{III}}/F_{\text{N}_2} > 1$

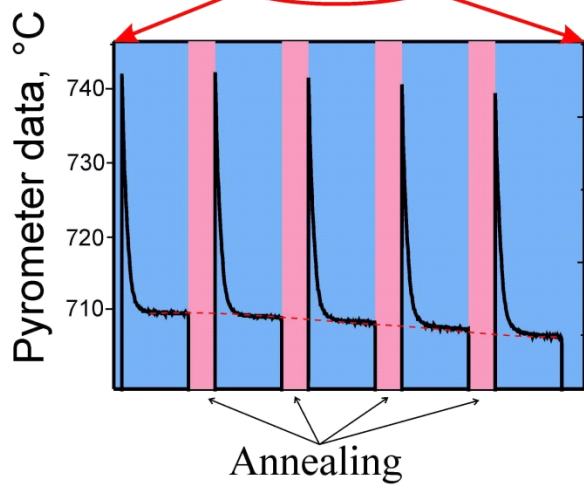
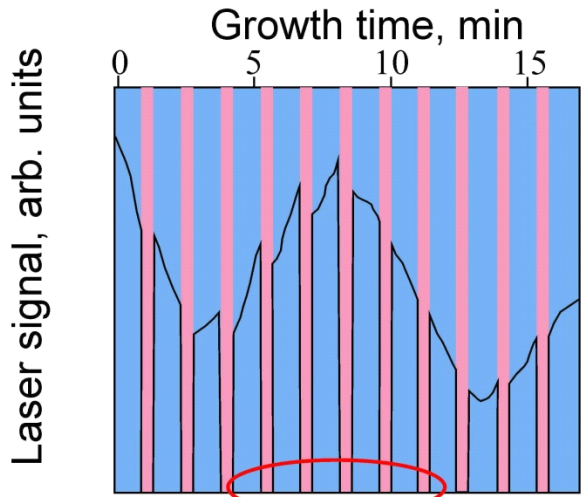
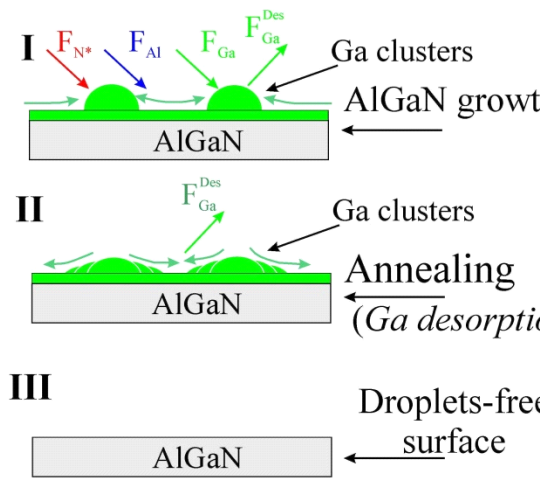
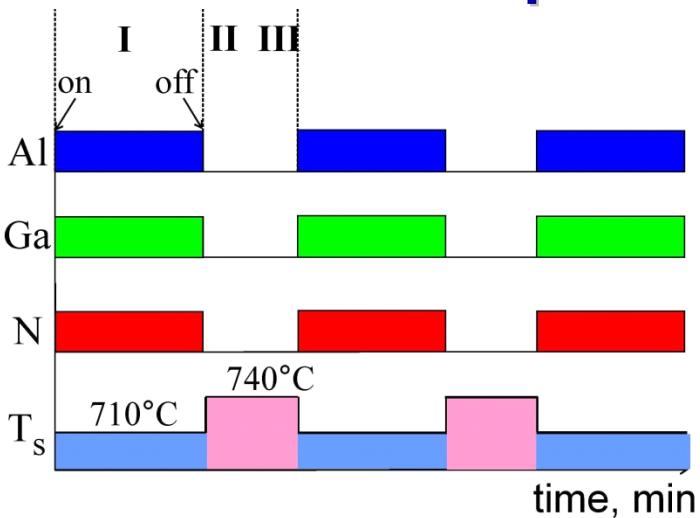
3D  $\rightarrow$  2D transition  
 occurs at constant  $F_{\text{Ga}}$

$E_{\text{Al-N}} > E_{\text{Ga-N}}, F_{\text{D}}^{\text{Al}} = 0$

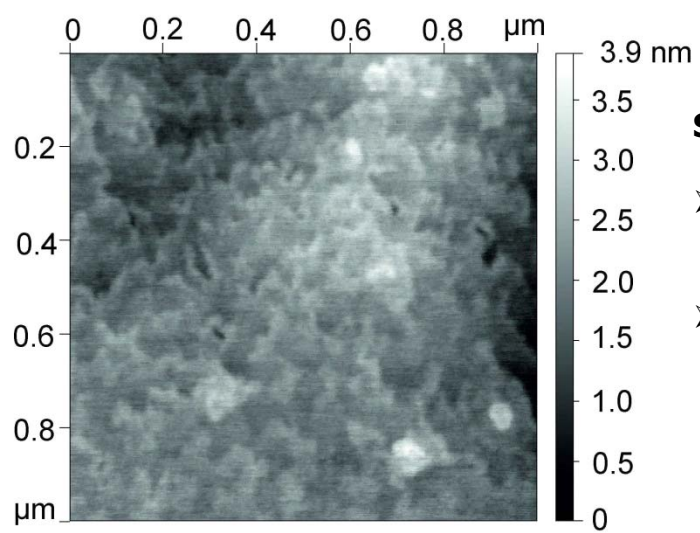
Growth kinetics is determined by Ga/N ratio and  $T_s$   
 but independent of the aluminum flux ( $F_{\text{Al}} < F_{\text{N}}$ )



# Metal-rich growth of thick 2D-AlGa<sub>N</sub> layers with temperature and flux modulated epitaxy



AFM images of the Al<sub>0.61</sub>Ga<sub>0.39</sub>N layer



**Special cares:**

- Interruption under N results in Ga<sub>N</sub> periodical insertions
- Growth of AlGa<sub>N</sub> on overheated wafer leads to Al-rich AlGa<sub>N</sub> periodical insertions

rms=0.47 nm

by closing the main shutter

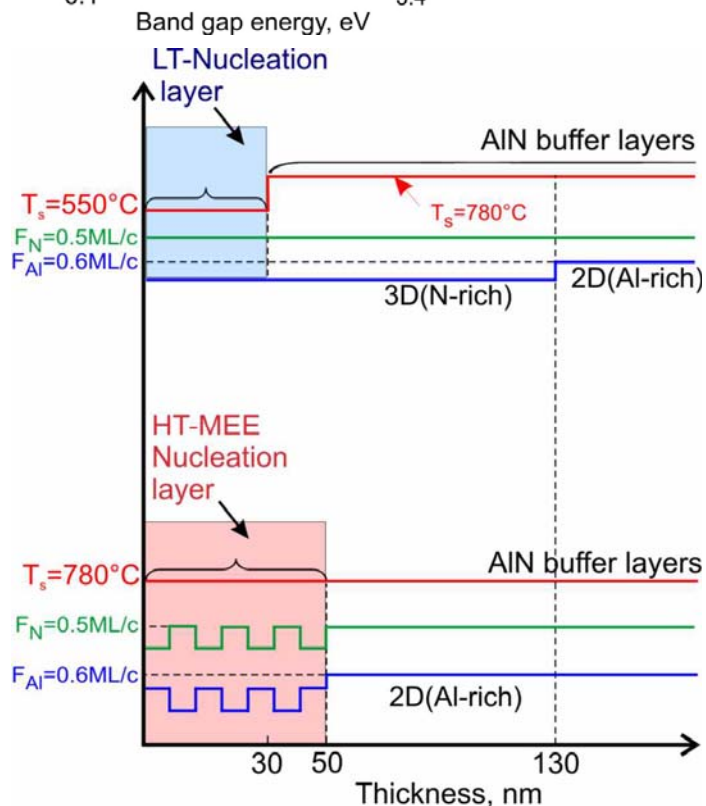
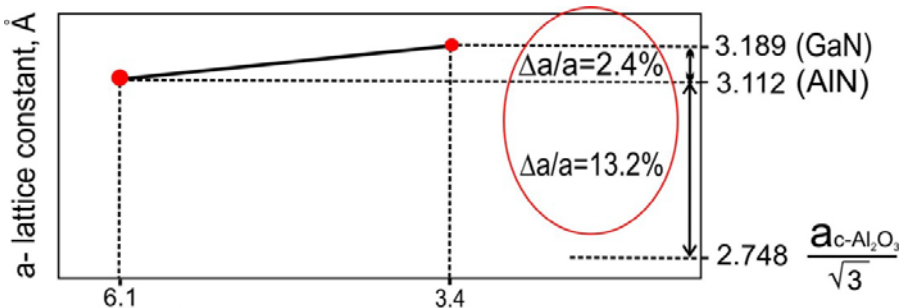


# Outline

- Applications of UV-optoelectronics and state-of-the-art of AlGaN-based UV LED and laser structures obtained by both MOVPE and PA MBE
- PA MBE growth and surface morphology control of III-Nitrides
  - Al-rich growth of thick AlN/c-Al<sub>2</sub>O<sub>3</sub> buffer layers
  - Growth kinetics of AlGaN layers (2D-3D transition)
- **Dislocation control and filtering in AlGaN/AlN/c-Al<sub>2</sub>O<sub>3</sub> heterostructures**
- Sub-monolayer Digital Alloying growth of Al<sub>x</sub>Ga<sub>1-x</sub>N/Al<sub>y</sub>Ga<sub>1-y</sub>N QWs
- Strain engineering in AlGaN QW heterostructures to prevent TE/TM switching of photoluminescence polarization
- Low-threshold optically pumped QW laser structures in the 258-303 nm range
- LEDs and solar-blind p-i-n photodiodes
- Conclusions

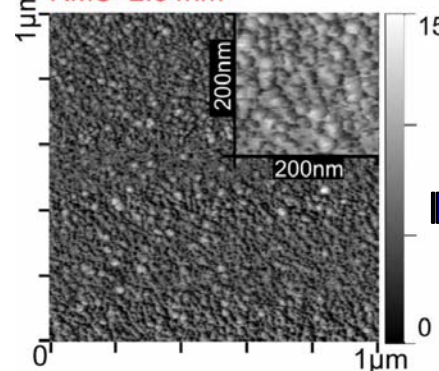


# Growth of AlN nucleation layers on c-Al<sub>2</sub>O<sub>3</sub> substrates at the different substrate temperatures & stoichiometric conditions



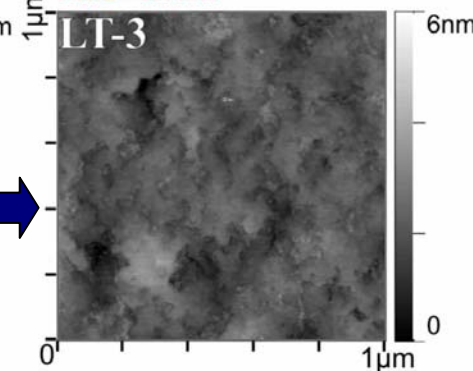
30nm-thick LT-AlN/c-Al<sub>2</sub>O<sub>3</sub>

RMS=2.34nm



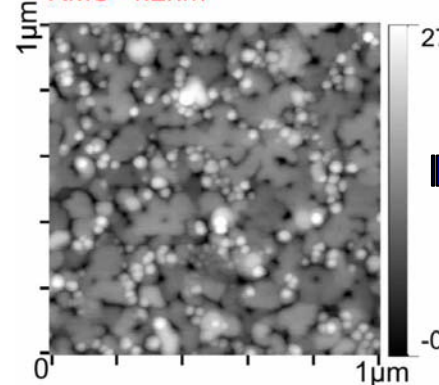
390nm-thick HT-AlN/LT-AlN/c-Al<sub>2</sub>O<sub>3</sub>

RMS=0.7nm



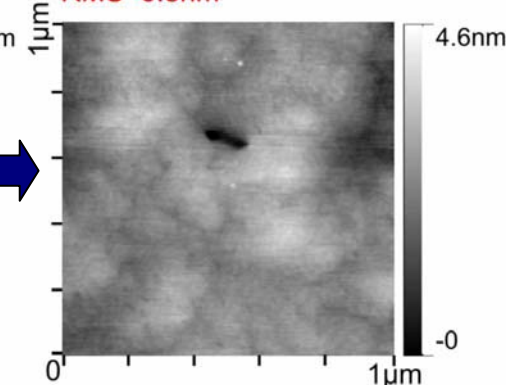
50nm-thick HT-MEE-AlN

RMS=4.2nm



390nm-thick HT-MEE-AlN

RMS=0.8nm



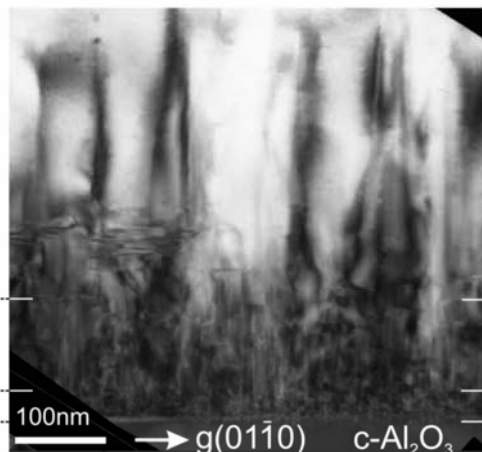
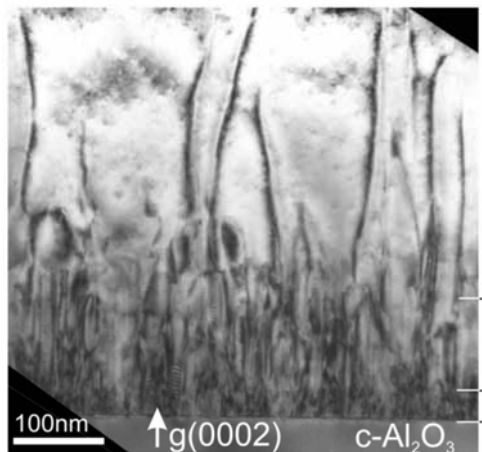
Nechaev et al., MBE-2012, J. Cryst. Growth, online 5 January 2013



# Lowering the TDs density in AlN/c-Al<sub>2</sub>O<sub>3</sub> heterostructure by changing stoichiometric conditions 3D→2D

screw & mixed

edge

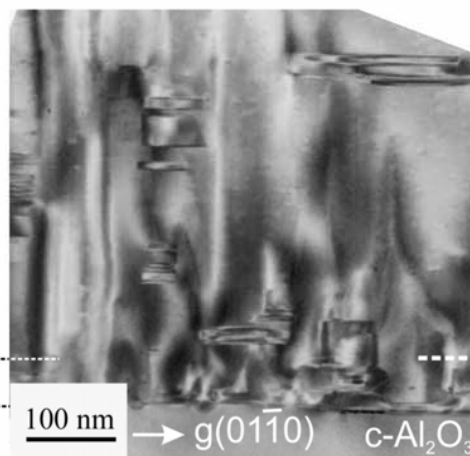
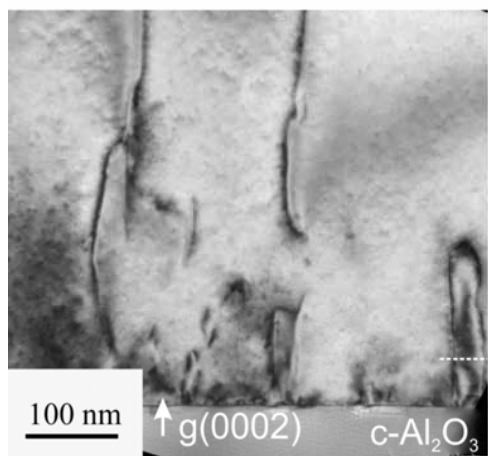
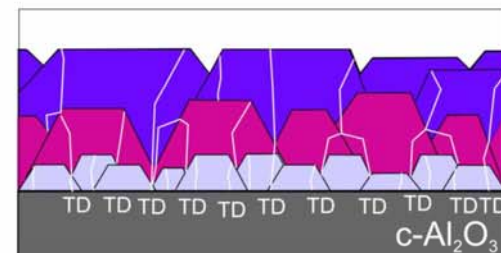


2D-HT-AlN layer (780°C)

3D-HT-AlN layer (780°C)

3D-LT-AlN nucleation layer (570°C)

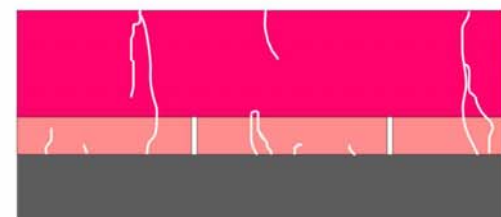
$$N_{TD} \sim 10^{10} \text{cm}^{-2}$$



2D-HT-AlN (780°C)

HT-MEE AlN

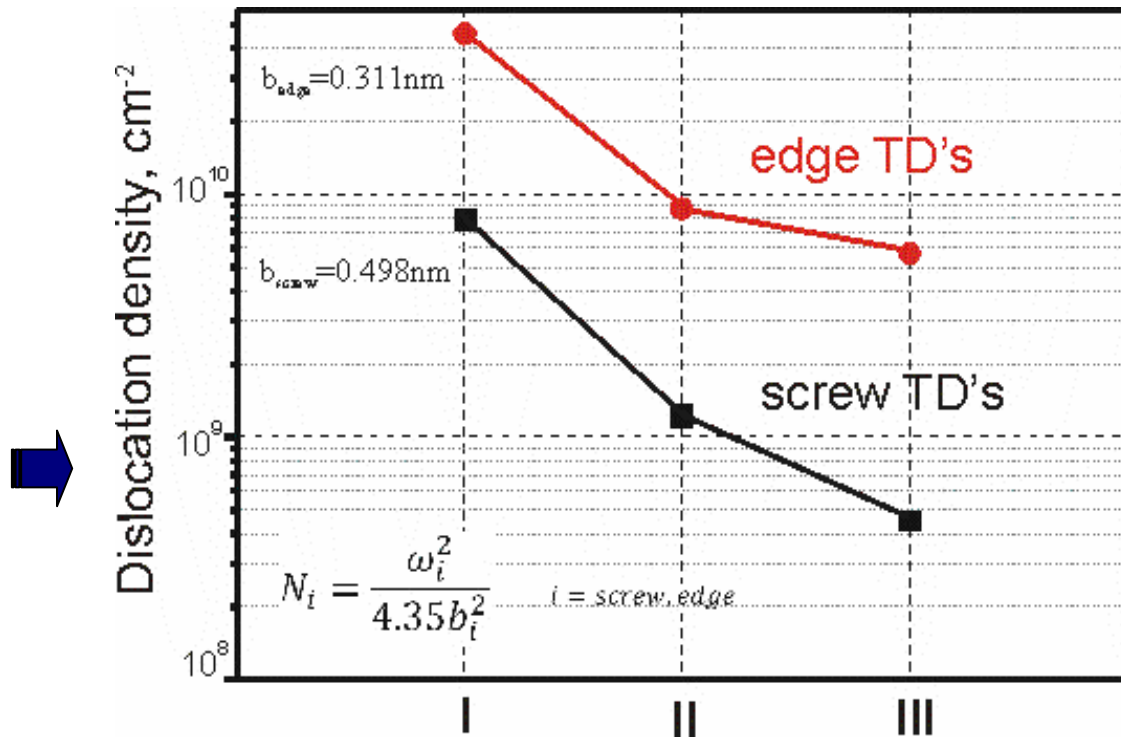
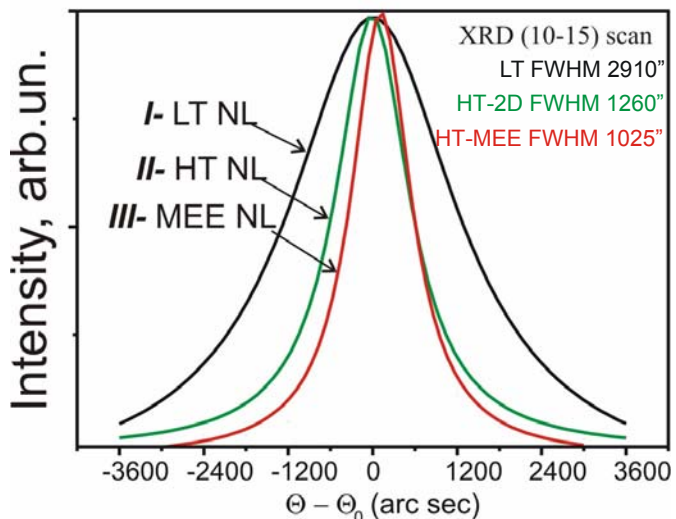
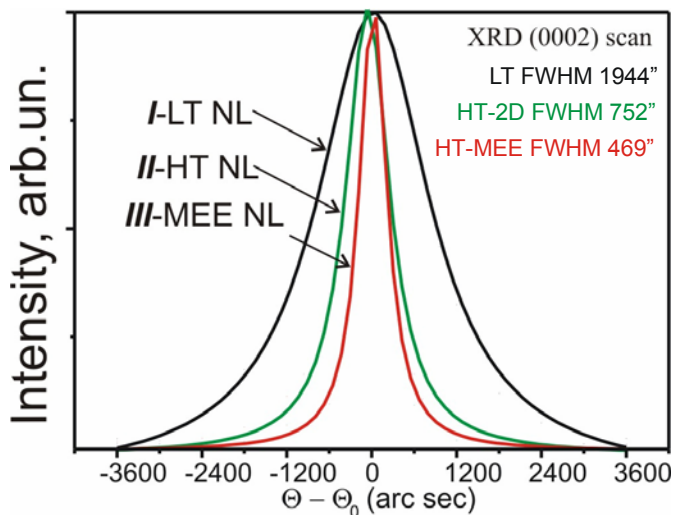
$$N_{TD} < 10^{10} \text{cm}^{-2}$$





# TDs density in 390-nm-thick AlN/c-Al<sub>2</sub>O<sub>3</sub> heterolayers with different nucleation layers (NL)

## XRD rocking curves

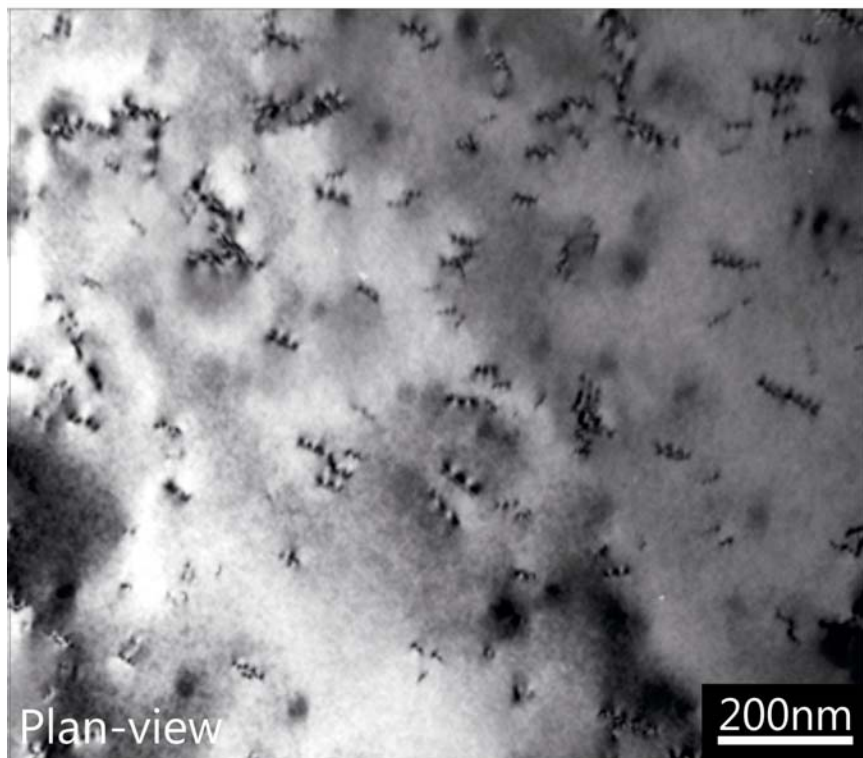
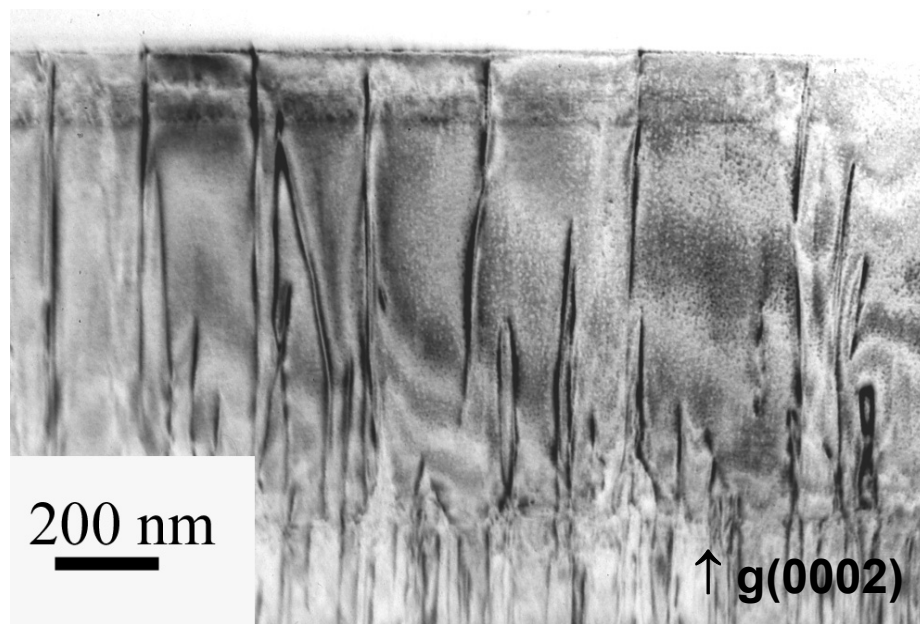


- I - Low T (570°C) 30-nm-thick AlN-NL+ pulse-AlN-BL(360nm)
- II - High T (760°C) 30-nm-thick AlN-NL + pulse-AlN-BL(360nm)
- III - MEE of 50-nm-thick HT-AlN + pulse-AlN-BL(340nm)



# General TEM view of AlGa<sub>0.6</sub>N/AlN/c-Al<sub>2</sub>O<sub>3</sub> SQW structure with NL grown in regime III

TEM

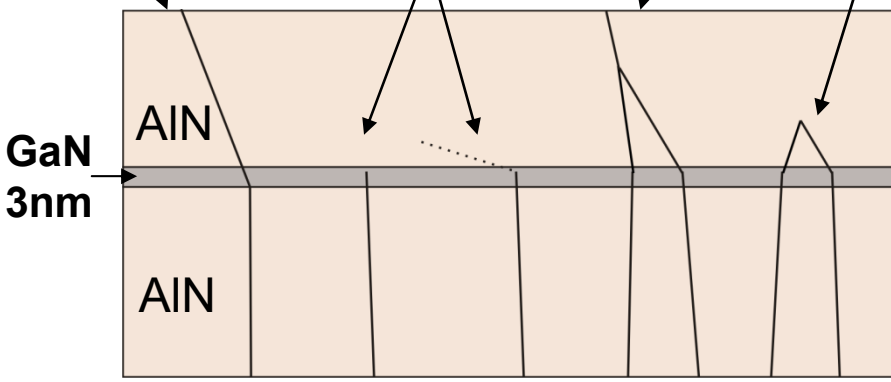


**TDD Screw:  $\sim 4 \cdot 10^8 \text{cm}^{-2}$**   
**Edge & Mixed:  $\sim 6 \cdot 10^9 \text{cm}^{-2}$**



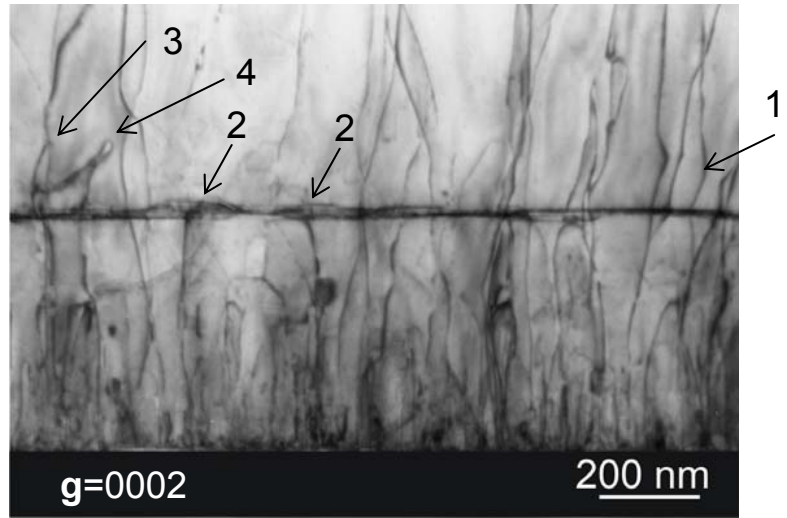
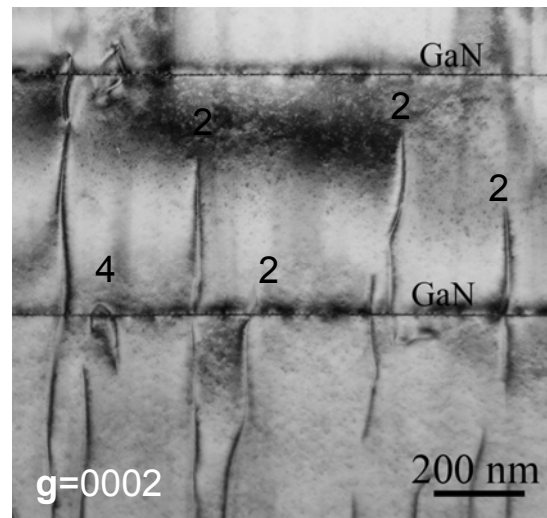
# Filtering TD densities in thick AlN buffer layers by multiple compressively-strained 3nm-thick GaN layers

1- inclination    2- blocking (redirection)    3- fusion    4- annihilation

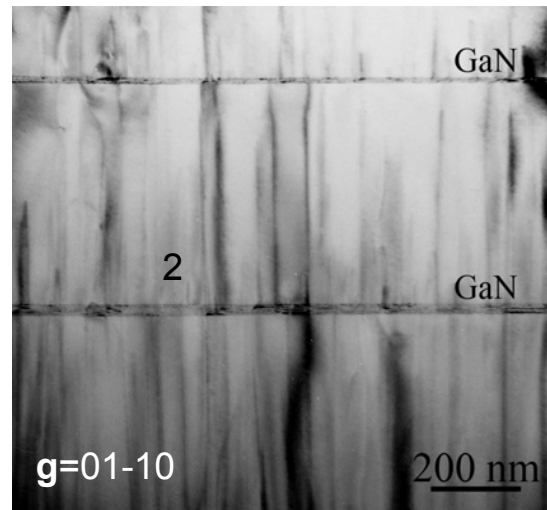


**AIN 2D mode**

$$N_{\text{screw}} = 3.5 \cdot 10^9 \text{ cm}^{-2}$$



$$N_{\text{edge}} \sim 10^{10} \text{ cm}^{-2}$$



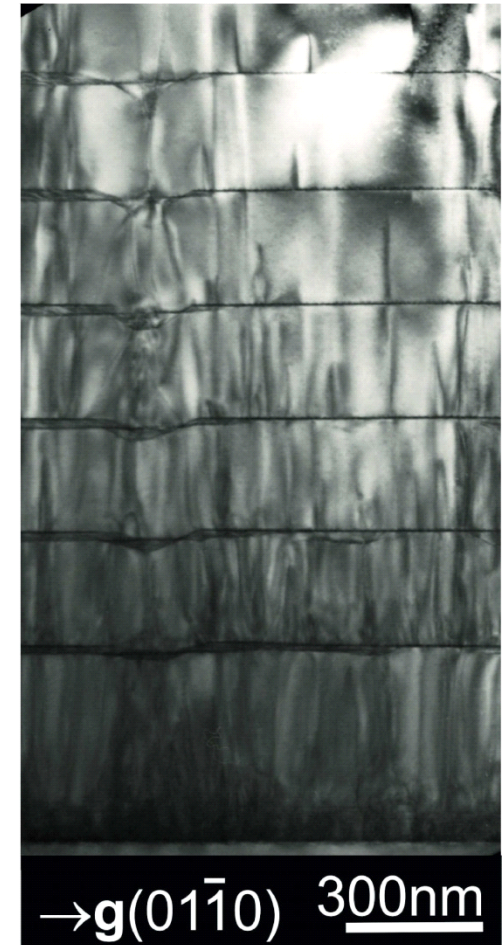
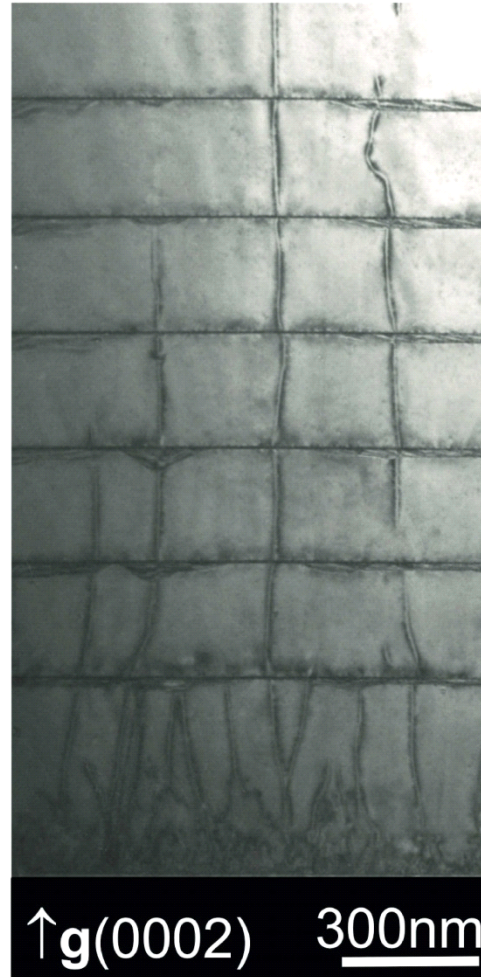
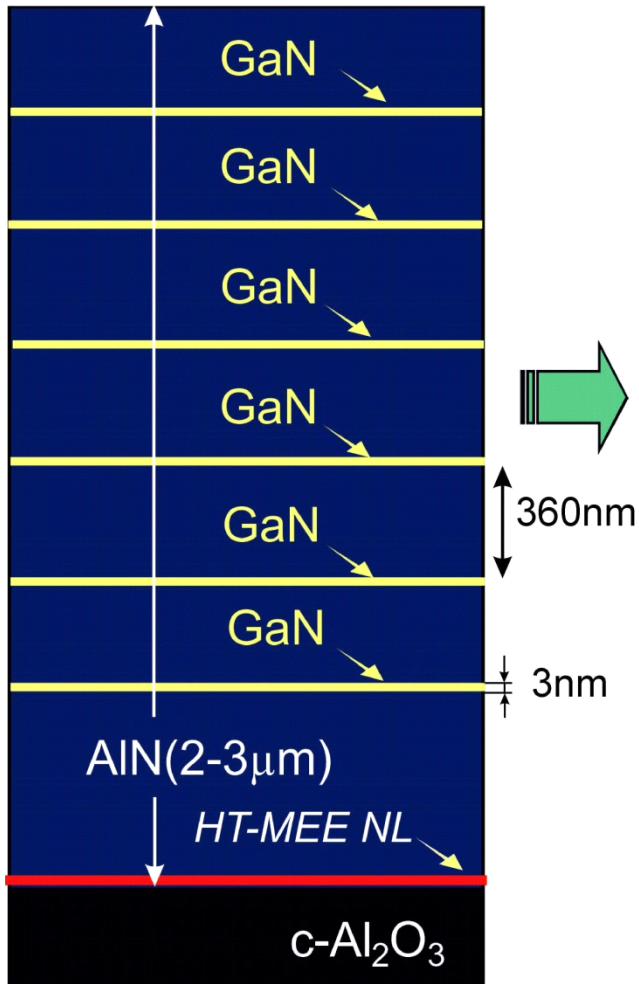
MOVPE results



J. Bai et al., Appl. Phys. Lett. **88**, 051903 (2006).  
 H. Jiang et al., Appl. Phys. Lett. **87**, 241911 (2005).

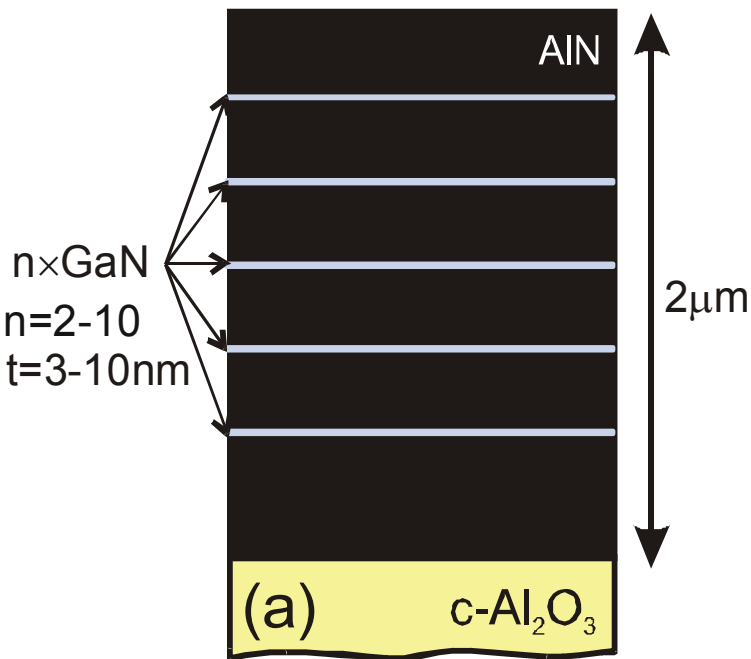


# Filtering TDs in thick AlN buffer layers by multiple compressively-strained 3nm-thick GaN layers

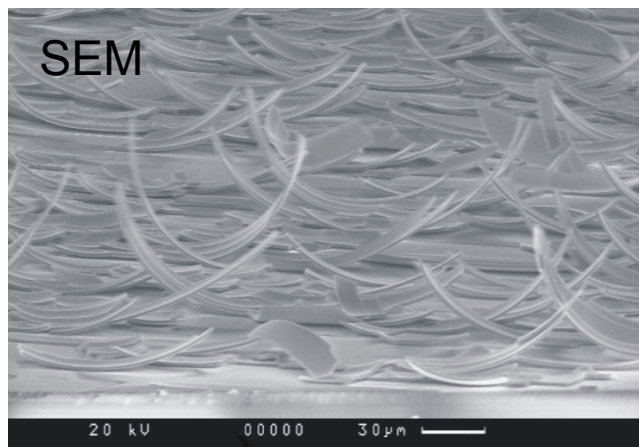




# Microscope images of the 2- $\mu\text{m}$ -thick GaN/AlN heterostructures with GaN interlayers of non-optimized design and growth conditions

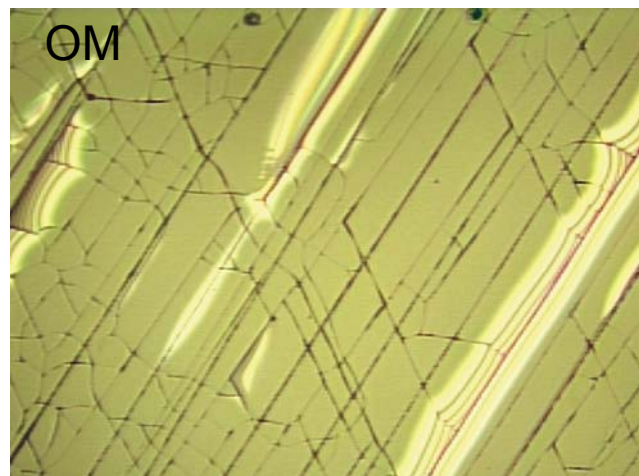


detachment



- 2D GaN growth mode
- multiple GaN interlayers above 6 interlayers
- for interlayer spacing smaller than 150nm even above 3 interlayers

cracking



- 3D GaN growth mode
- multiple GaN interlayers at small spacing below 150 nm



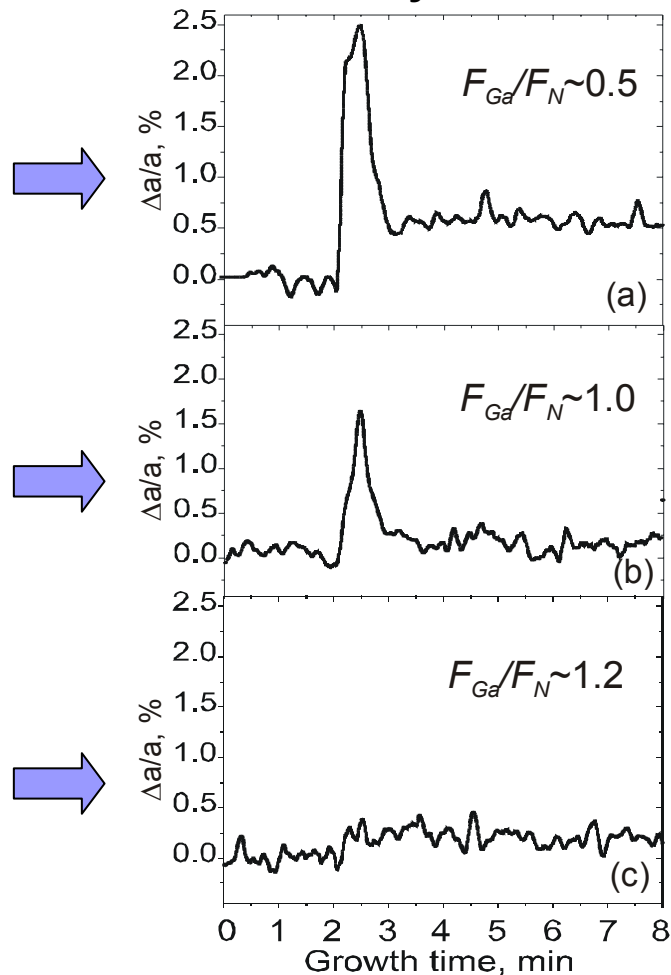
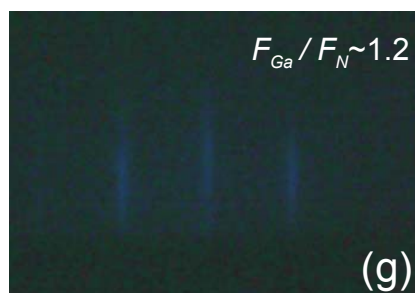
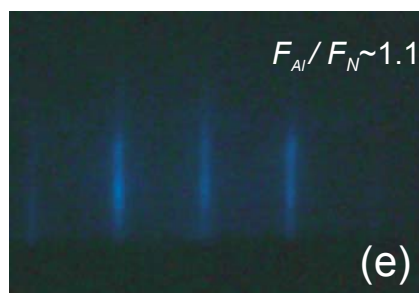
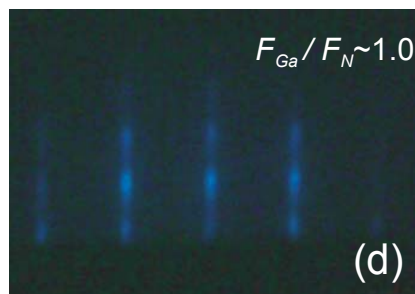
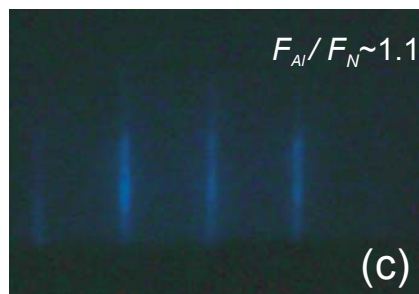
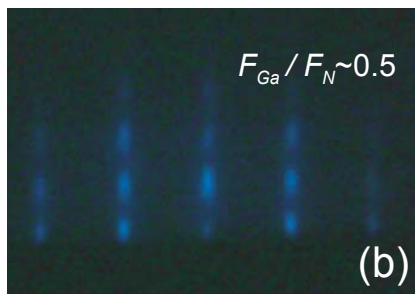
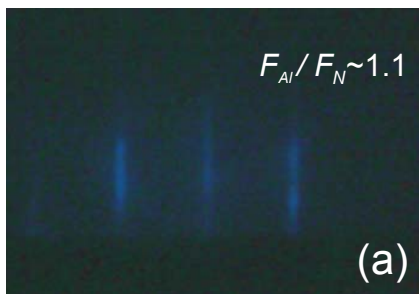
# Strain relaxation versus surface morphology of 3-nm-thick GaN interlayers in 2D AlN buffer

RHEED patterns during growth

Temporal changes of a-lattice constant during growth of GaN interlayers

Al-rich AlN buffer

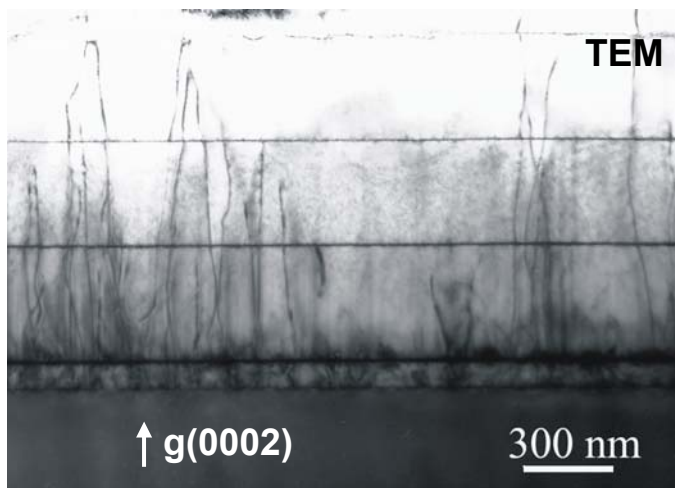
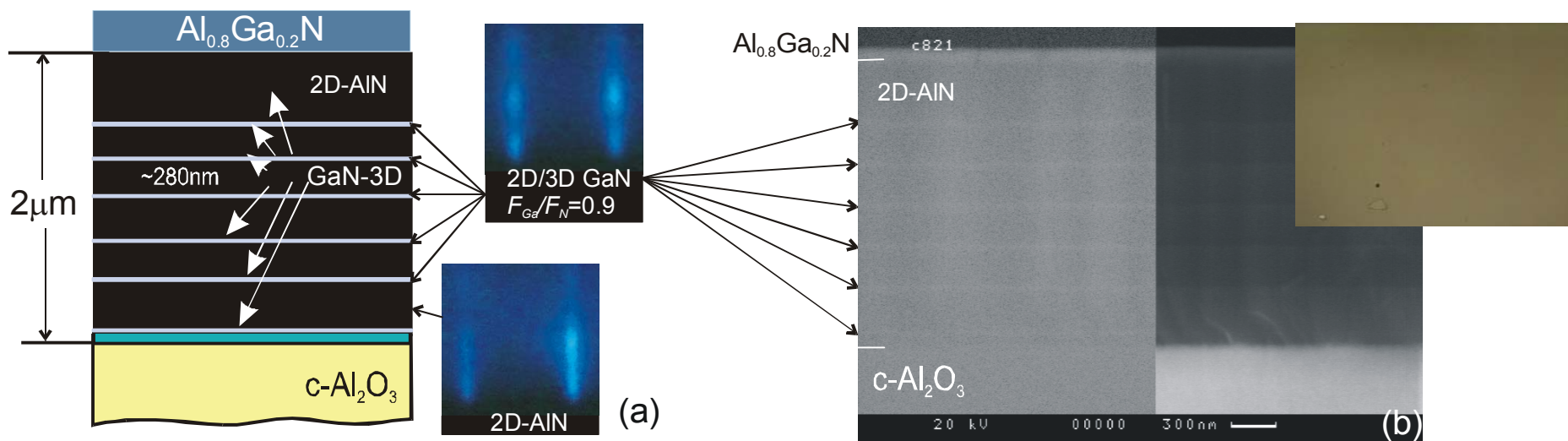
GaN interlayer



In accordance with model by Daudin's group  
[Phys. Rev. B **63**, 245307 (2001), J. Appl. Phys. **95**, 1127 (2004)]



# Structural property of $\text{Al}_{0.8}\text{Ga}_{0.2}\text{N}(100\text{nm})/\text{AlN}(2\mu\text{m})/\text{c-Al}_2\text{O}_3$ heterostructure grown on optimized AlN/GaN buffer

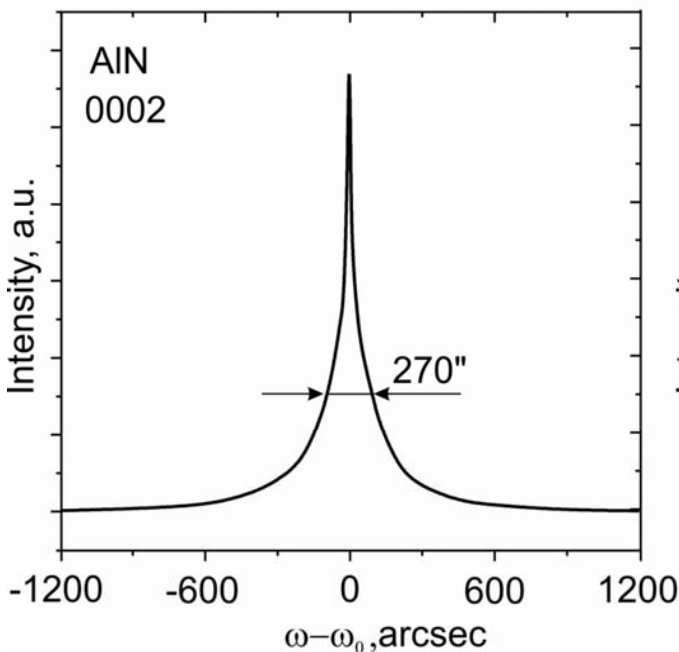


- Metal-flux modulated Al-rich growth of 260-nm-thick AlN layers separated by six 3-nm-thick GaN interlayers grown under the slightly N-rich conditions ( $F_{\text{Ga}}/F_{\text{N}}\sim 0.9$ ).
- Screw&mixed TD density reduced to  $\sim 10^8 \text{ cm}^{-2}$

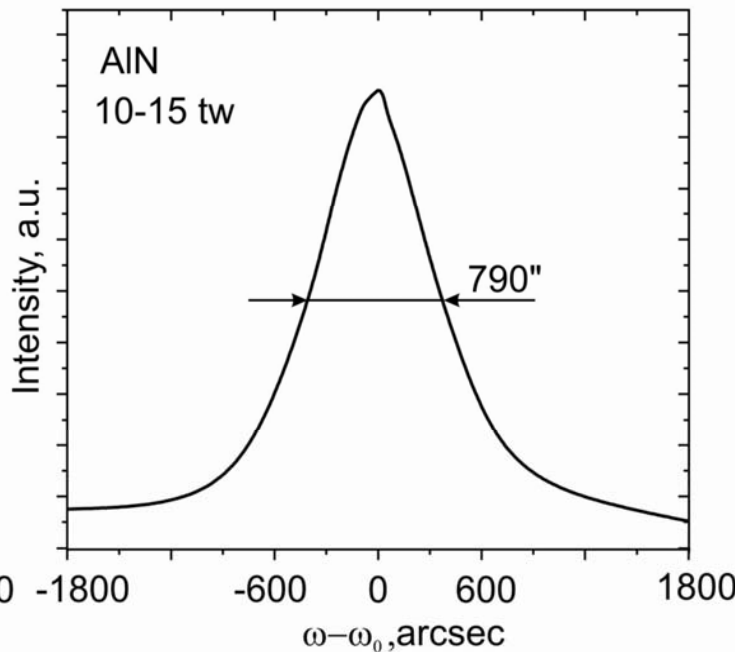


# XRD rocking curves of AlN buffer layer in SQW structure grown on c-sapphire at optimized AlN/GaN buffer structure design and growth conditions

symmetric (0002) reflex



skew-symmetric (10-15tw) reflex



**Screw TD :  $\sim 1.5 \cdot 10^8 \text{cm}^{-2}$**

**Edge & Mixed TD :  $\sim 3 \cdot 10^9 \text{cm}^{-2}$**

$$N_{\text{TD}} = w^2 / 4.35b^2$$

**AlN:**

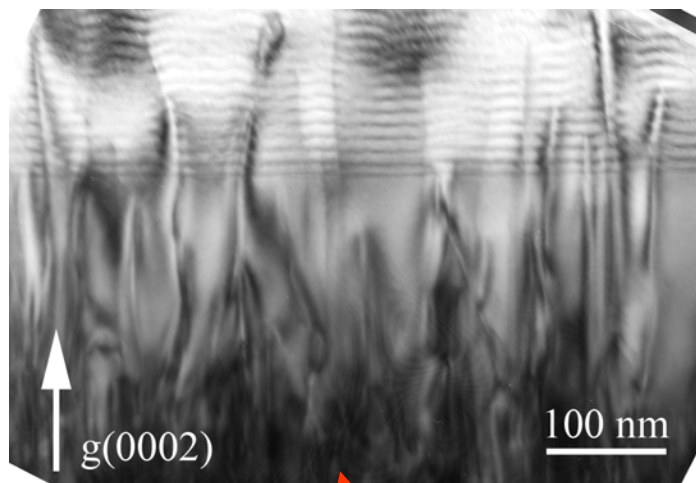
**b = 0.498 nm (for screw TD)**

**b = 0.311 nm (for edge TD)**

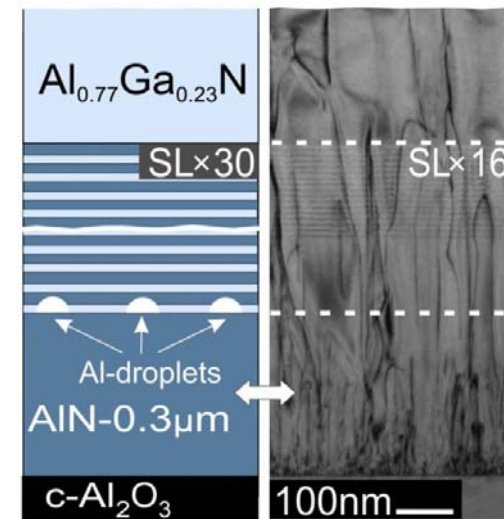
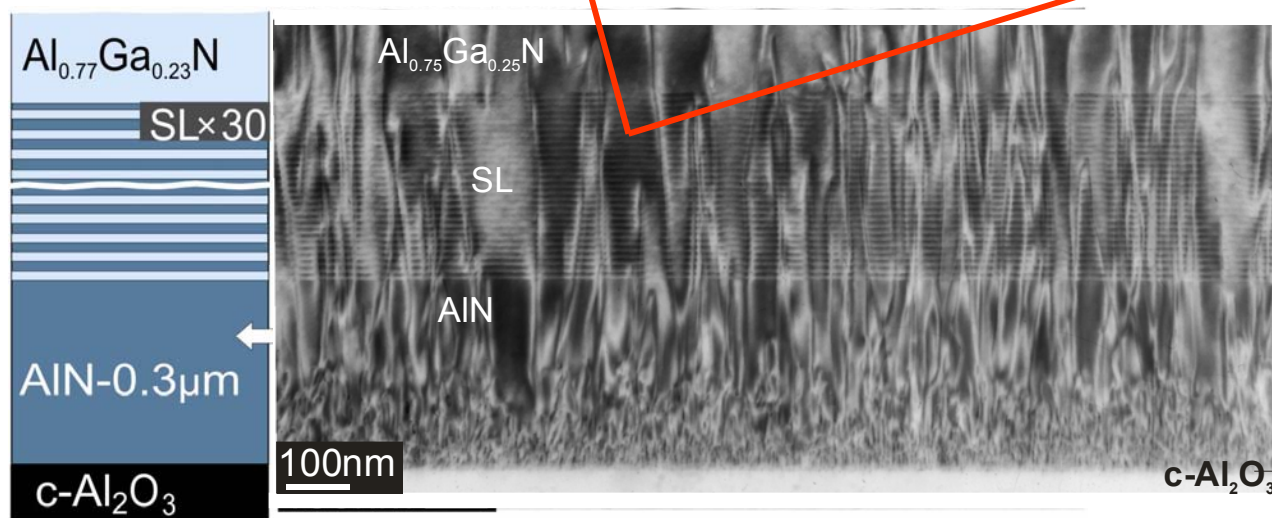
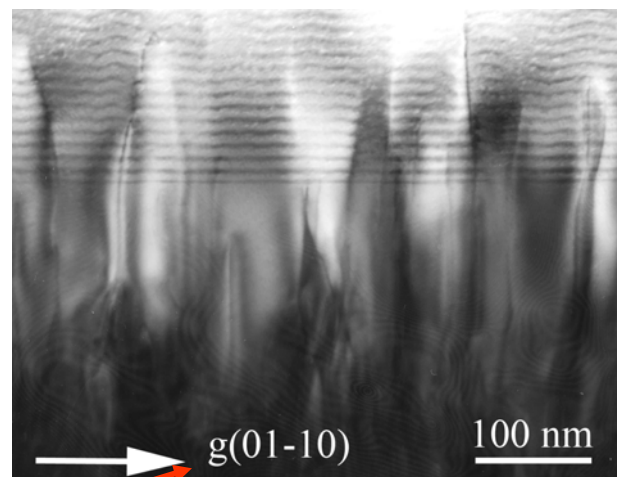


# Suppression of TDs by using 30x{Al<sub>0.77</sub>Ga<sub>0.23</sub>N/AlN}/AlN superlattices ( $T = 10\text{nm}$ , $x_{av} = 0.9$ )

screw & mixed



edge



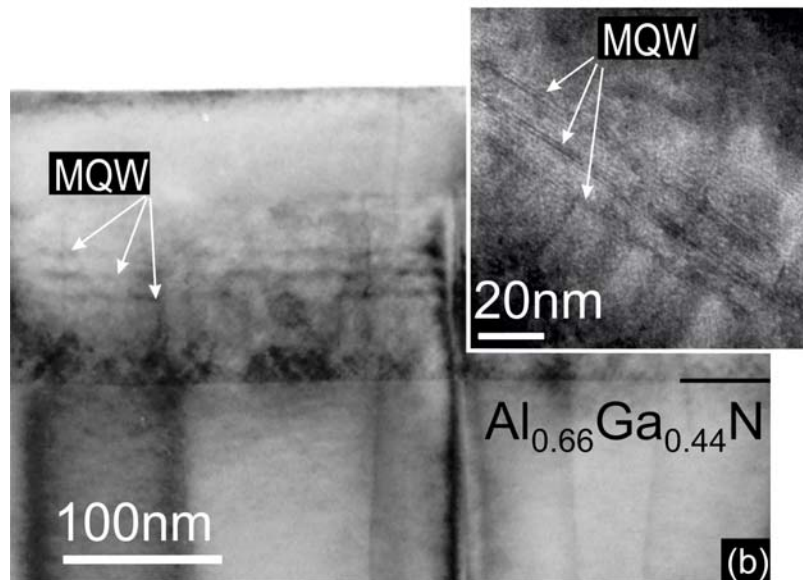
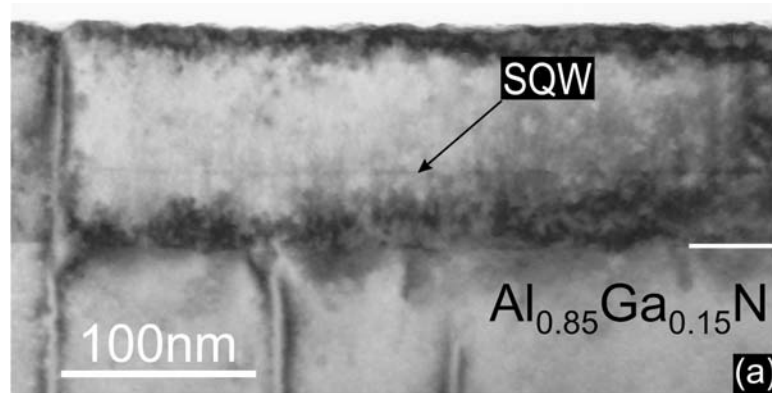
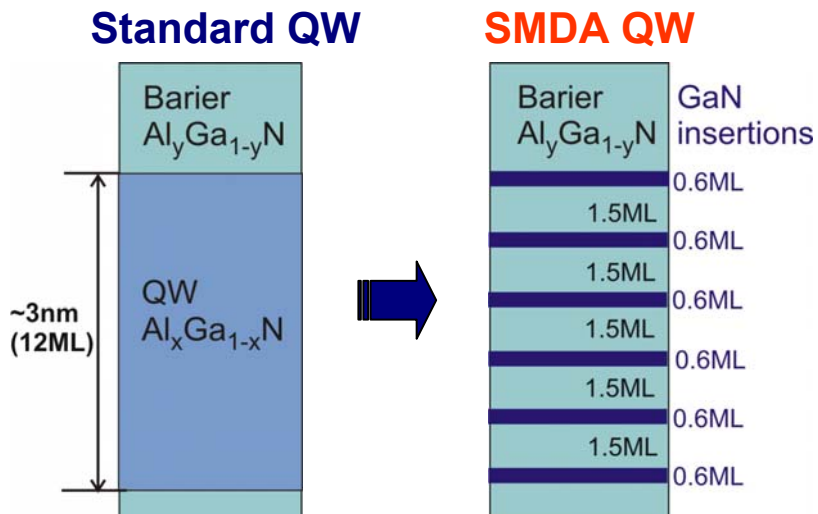


# Outline

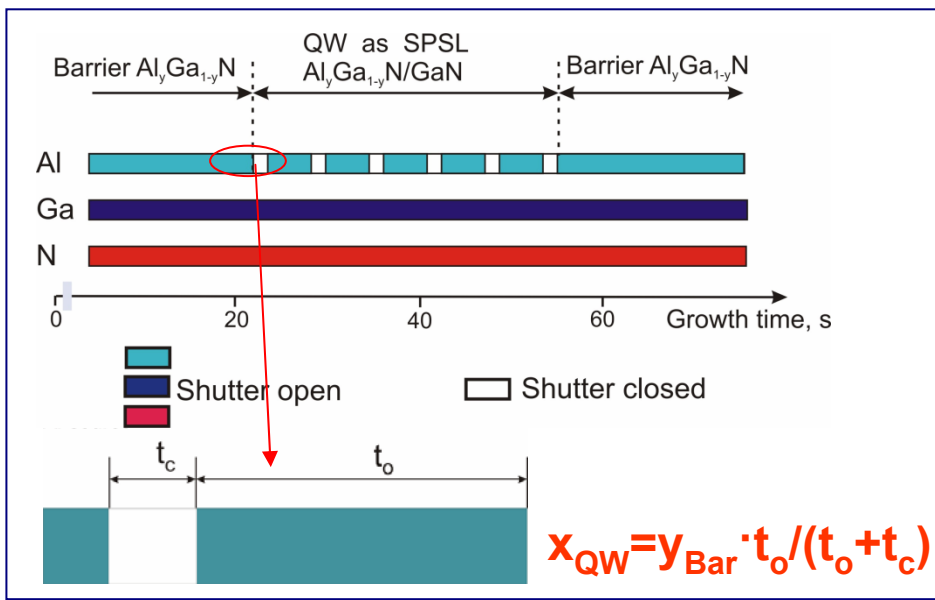
- Applications of UV-optoelectronics and state-of-the-art of AlGaN-based UV LED and laser structures obtained by both MOVPE and PA MBE
- PA MBE growth and surface morphology control of III-Nitrides
  - Al-rich growth of thick AlN/c-Al<sub>2</sub>O<sub>3</sub> buffer layers
  - Growth kinetics of AlGaN layers (2D-3D transition)
- Dislocation control and filtering in AlGaN/AlN/c-Al<sub>2</sub>O<sub>3</sub> heterostructures
- **Sub-monolayer Digital Alloying growth of Al<sub>x</sub>Ga<sub>1-x</sub>N/Al<sub>y</sub>Ga<sub>1-y</sub>N QWs**
- Strain engineering in AlGaN QW heterostructures to prevent TE/TM switching of photoluminescence polarization
- Low-threshold optically pumped QW laser structures in the 258-303 nm range
- LEDs and solar-blind p-i-n photodiodes
- Conclusions



# Submonolayer Digital Alloying (SMDA) growth of $\text{Al}_x\text{Ga}_{1-x}\text{N}/\text{Al}_y\text{Ga}_{1-y}\text{N}$ MQW heterostructures



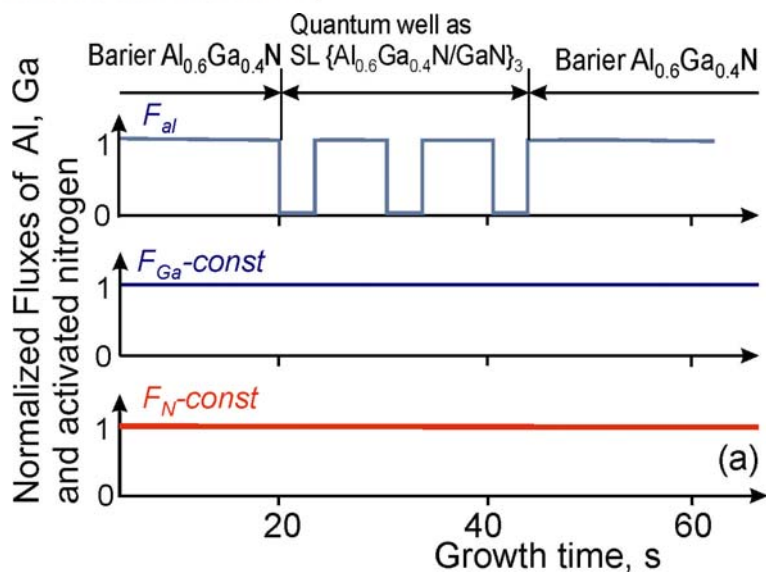
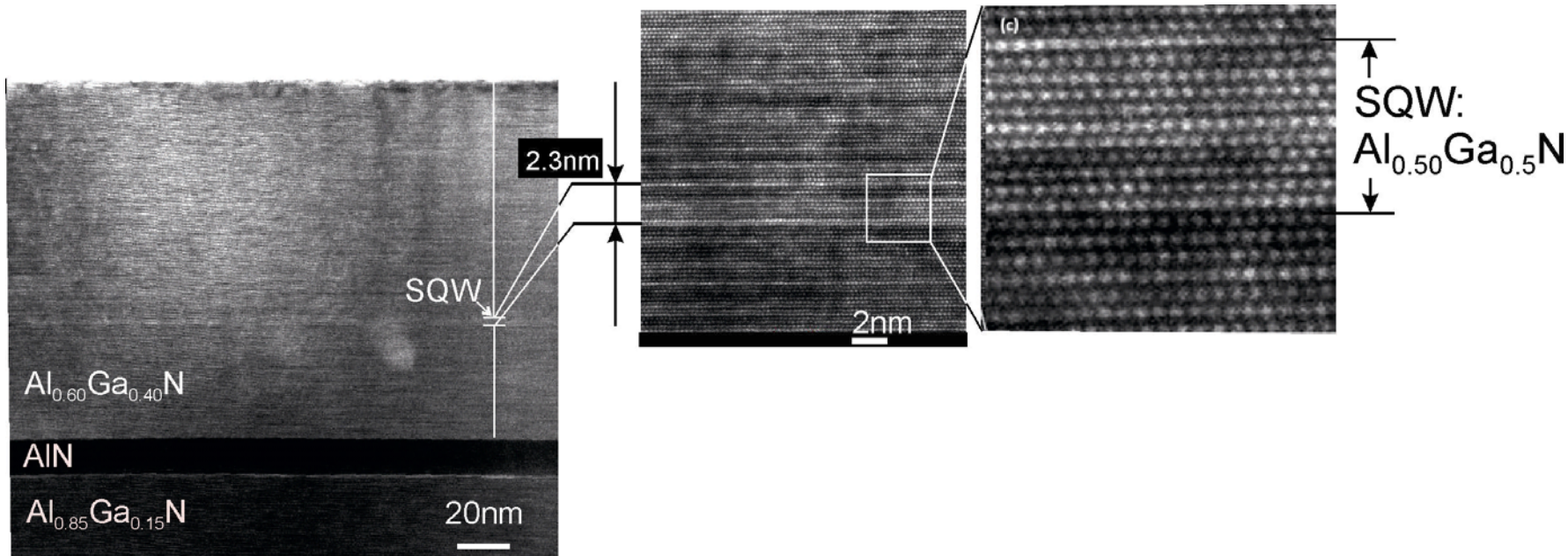
## Shutter control of Al content in AlGaN QW



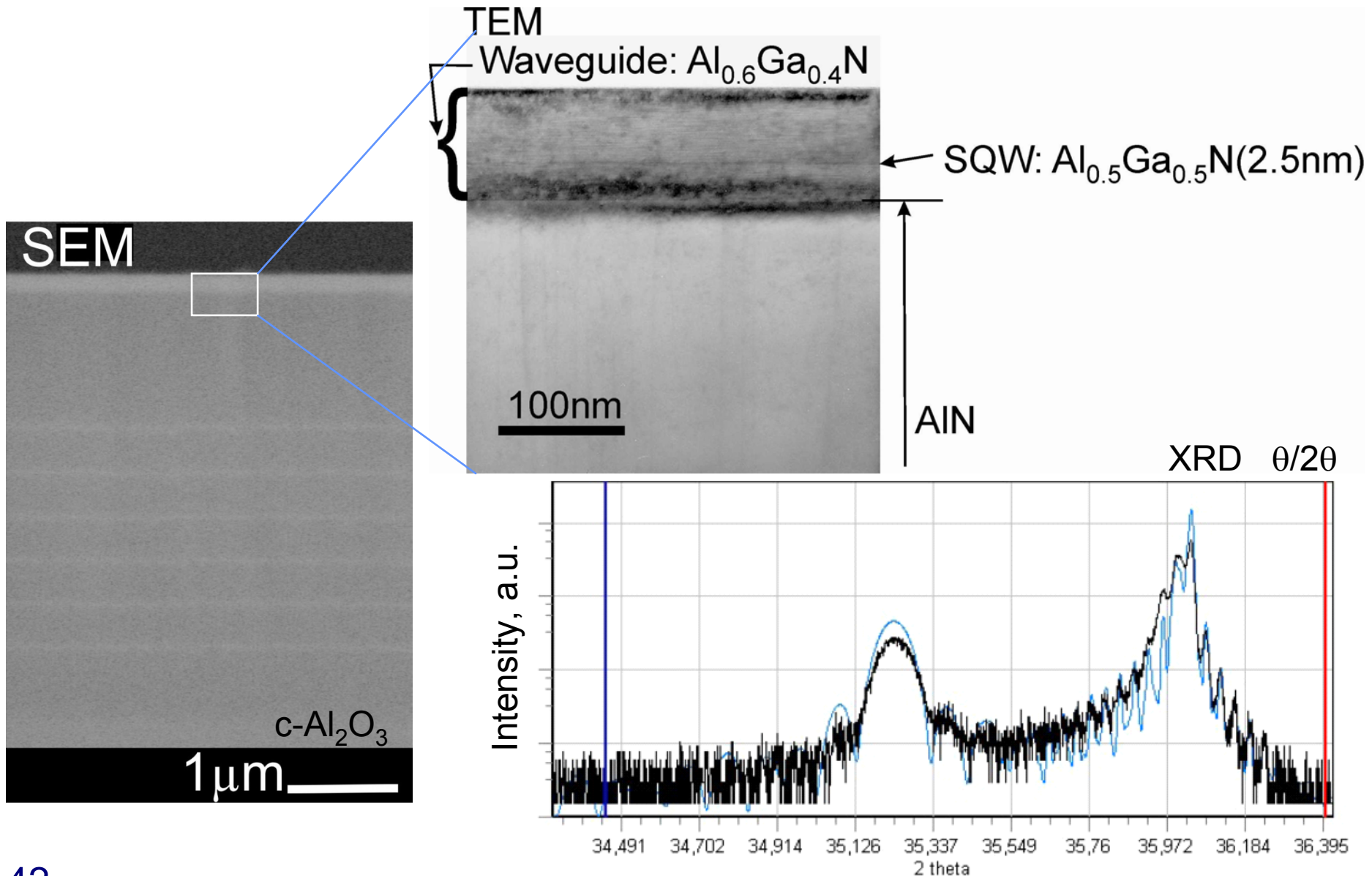
Jmerik et al., *Semiconductors* **42**, 1452, (2008),  
*PSS A* **210**, 439(2013).



# HAADF STEM and HRTEM images of AlGaN-based SQW heterostructure

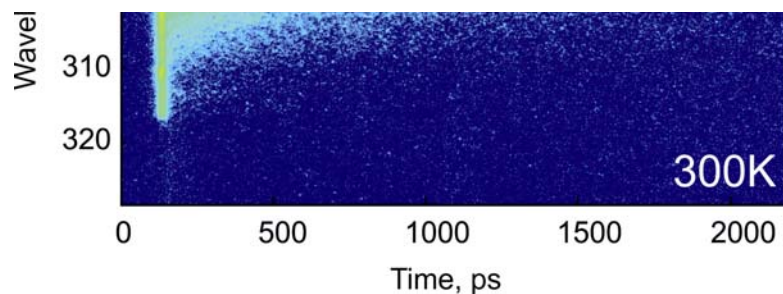
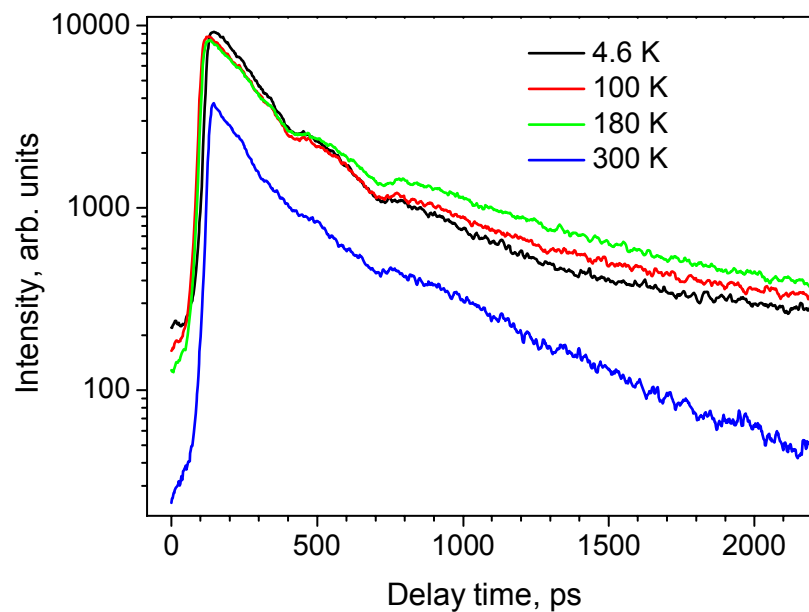
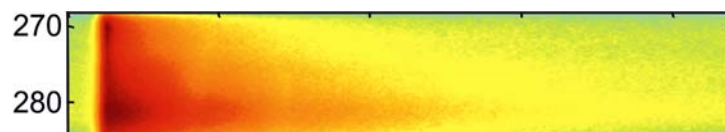
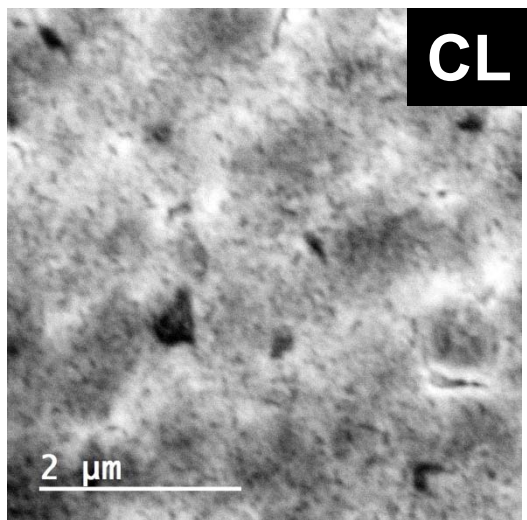
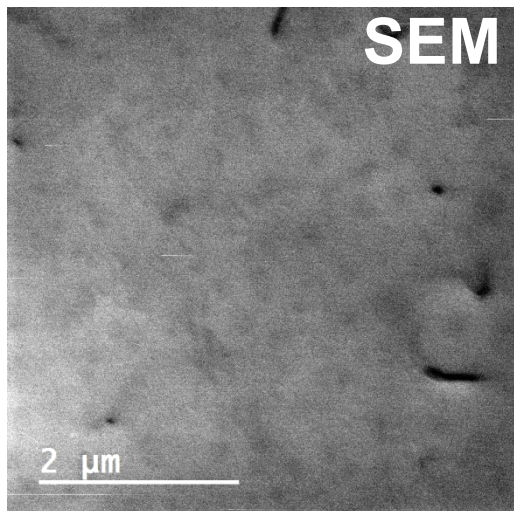


# Structural properties of AlGaN-based SQW heterostructure grown on c-Al<sub>2</sub>O<sub>3</sub>





# CL and TRPL spectra of $\text{Al}_{0.5}\text{Ga}_{0.5}\text{N}(2.5\text{nm})/\text{Al}_{0.6}\text{Ga}_{0.4}\text{N}$ SQW





# Outline

- Applications of UV-optoelectronics and state-of-the-art of AlGaN-based UV LED and laser structures obtained by both MOVPE and PA MBE
- PA MBE growth and surface morphology control of III-Nitrides
  - Al-rich growth of thick AlN/c-Al<sub>2</sub>O<sub>3</sub> buffer layers
  - Growth kinetics of AlGaN layers (2D-3D transition)
- Dislocation control and filtering in AlGaN/AlN/c-Al<sub>2</sub>O<sub>3</sub> heterostructures
- Sub-monolayer Digital Alloying growth of Al<sub>x</sub>Ga<sub>1-x</sub>N/Al<sub>y</sub>Ga<sub>1-y</sub>N QWs
- **Strain engineering in AlGaN QW heterostructures to prevent TE/TM switching of photoluminescence polarization**
- Low-threshold optically pumped QW laser structures in the 258-303 nm range
- LEDs and solar-blind p-i-n photodiodes
- Conclusions

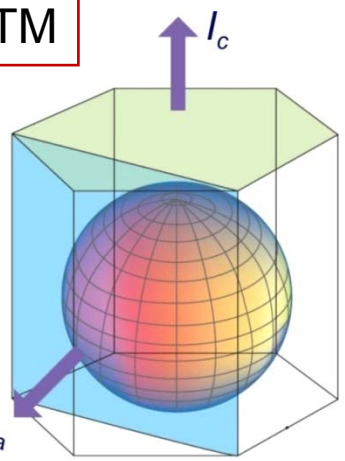
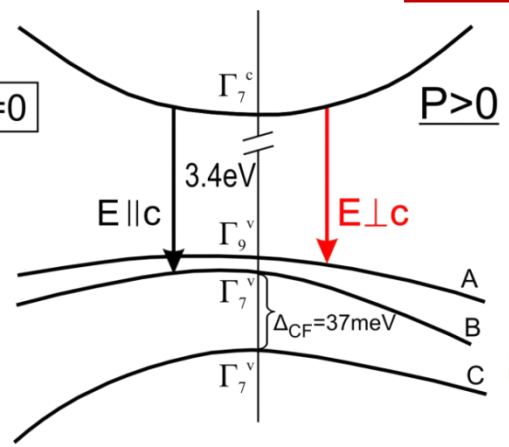


# Valence band structure of $\text{Al}_x\text{Ga}_{1-x}\text{N}$ ( $x=0-1$ ) alloys and anisotropic polarization of output UV radiation from GaN&AlN

## GaN

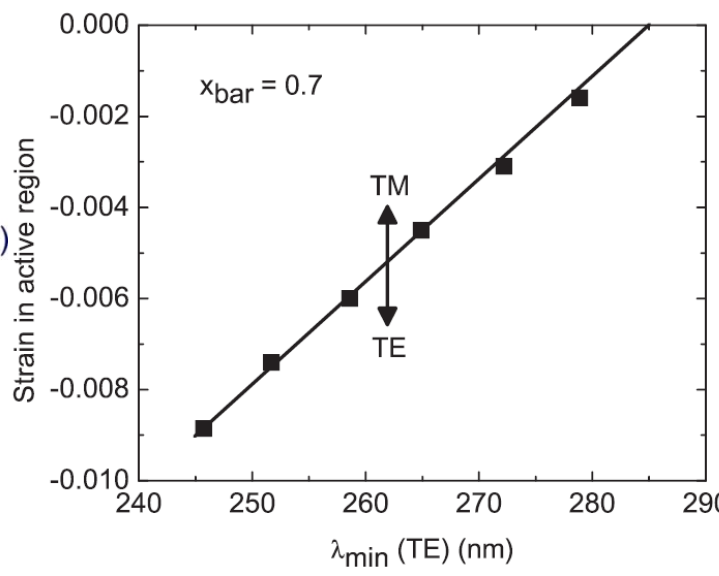
TE > TM

x=0



$$\frac{I_a}{I_c} = 1$$

GaN ( $\lambda=365\text{nm}$ )

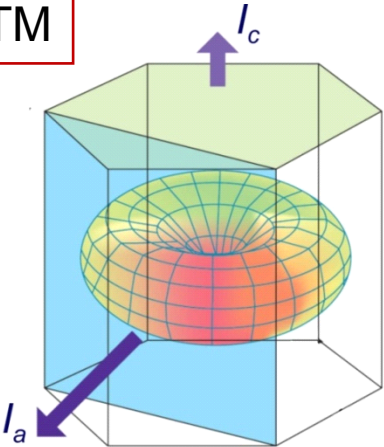
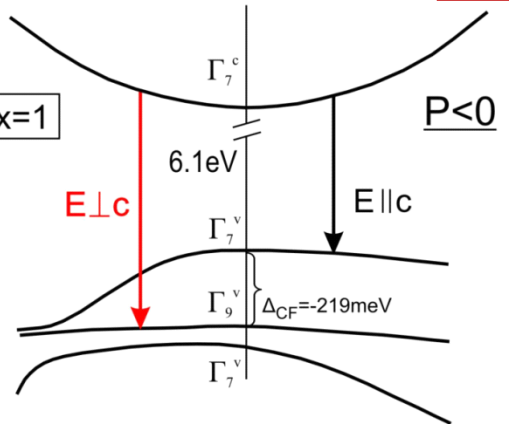


Northrup et al., *Appl.Phys.Lett.* **100**, 021101 (2012)  
 Durnev & Karpov, *Phys.Stat.Solids B* **250**, 180(2013)

## AlN

TE < TM

x=1



$$\frac{I_a}{I_c} = 25$$

AlN ( $\lambda=210\text{nm}$ )

### For TE polarization:

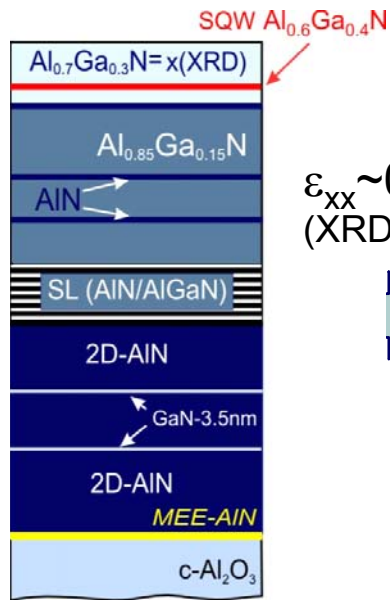
- Efficient light extraction from mid-UV LEDs normally to c-plane
- Higher differential gain in the mid-UV laser cavity due to the higher reflectivity coefficient

Nam et al., *APL* **84**, 5264 (2004).

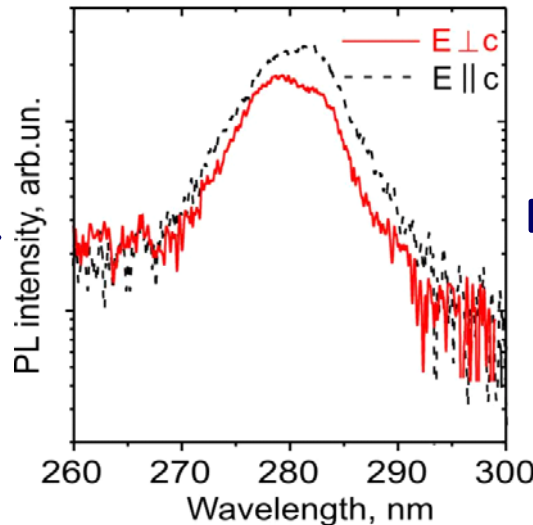
Taniyasu et al., *APL* **90**, 261911 (2007).



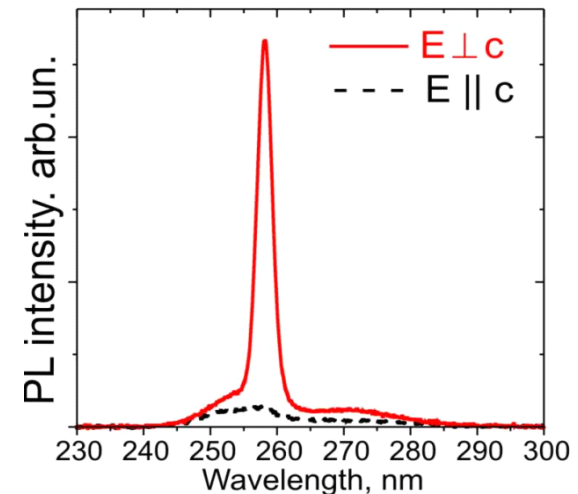
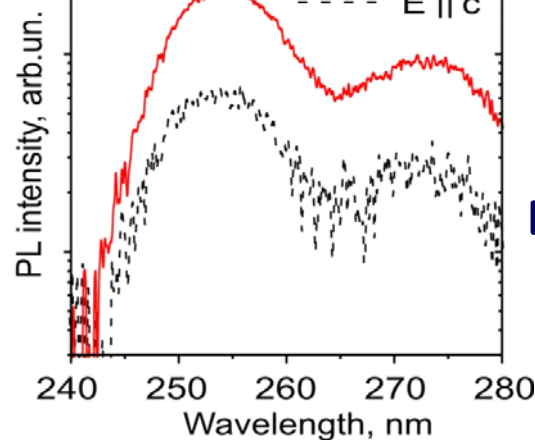
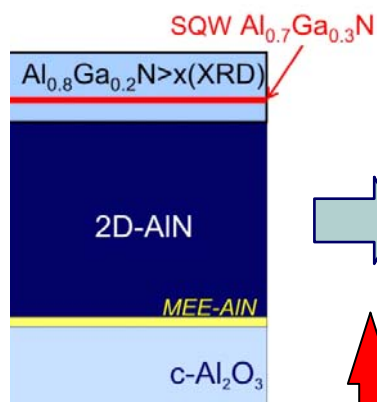
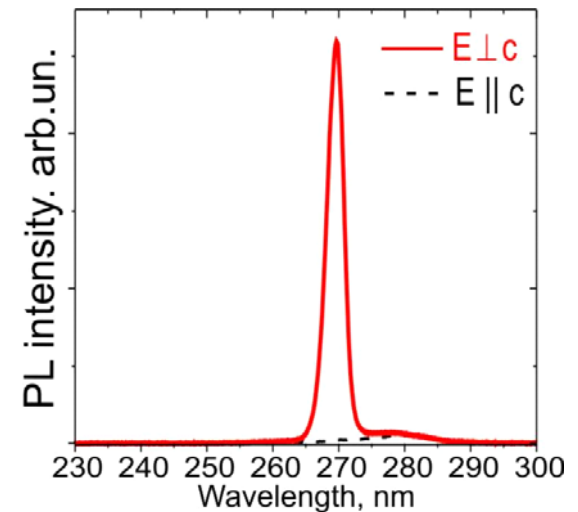
# PL spectra of AlGa<sub>x</sub>N-based heterostructures with the different compressive strains on c-Al<sub>2</sub>O<sub>3</sub>



Spontaneous PL spectra



Stimulated PL spectra



Lutsenko et al., *Physics of Solid State*, **55**(10), 2058, 2013

Northrup et al., *Appl. Phys. Lett.* **100**, 021101 (2012).

Peking University, May 15, 2014

$\epsilon_{xx} \sim -0.7-0.8\%$  in the Al<sub>x</sub>Ga<sub>1-x</sub>N SQW corresponds to theoretical estimations of the compressive strain necessary for suppression of the valence band crossover for  $x > 0.7$



# Kinetic limitations for generation of threading dislocations

Misfit dislocations generation rates  $\left( \frac{dN}{dt} \right)$  to be influenced by the:

- Stress due to misfit strain  $(\tau_{eff})$
- Density of nucleation sites  $(N_0)$  → **2D → Metal-rich PAMBE !**
- Growth temperature  $(T)$  → **Low T (<800°) PA MBE !**

This can be described by the semiempirical expression :

$$\frac{dN}{dt} = B \cdot N_0 \left( \frac{\tau_{eff}}{\mu} \right)^n \exp\left( -\frac{E_a}{kT} \right)$$

Houghton, J.Appl.Phys. 70, (1991), 2136

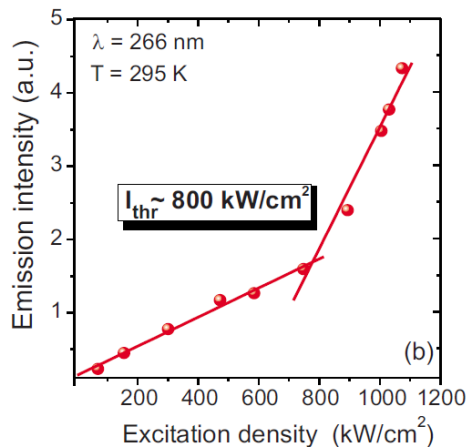
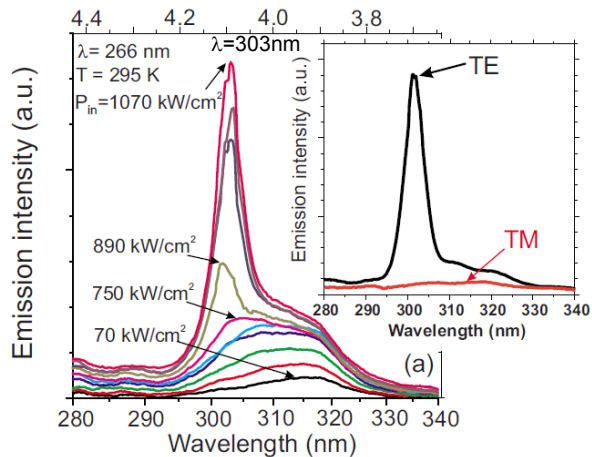


# Outline

- Applications of UV-optoelectronics and state-of-the-art of AlGaN-based UV LED and laser structures obtained by both MOVPE and PA MBE
- PA MBE growth and surface morphology control of III-Nitrides
  - Al-rich growth of thick AlN/c-Al<sub>2</sub>O<sub>3</sub> buffer layers
  - Growth kinetics of AlGaN layers (2D-3D transition)
- Dislocation control and filtering in AlGaN/AlN/c-Al<sub>2</sub>O<sub>3</sub> heterostructures
- Sub-monolayer Digital Alloying growth of Al<sub>x</sub>Ga<sub>1-x</sub>N/Al<sub>y</sub>Ga<sub>1-y</sub>N QWs
- Strain engineering in AlGaN QW heterostructures to prevent TE/TM switching of photoluminescence polarization
- **Low-threshold optically pumped QW laser structures in the 258-303 nm range**
- LEDs and solar-blind p-i-n photodiodes
- Conclusions



# Optically pumped mid-UV lasing in AlGaIn heterostructures grown by PA MBE (previous results)



APPLIED PHYSICS LETTERS 96, 141112 (2010)

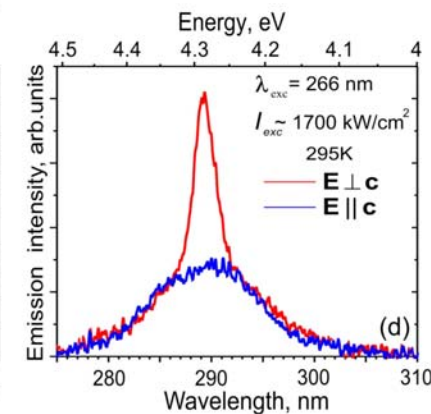
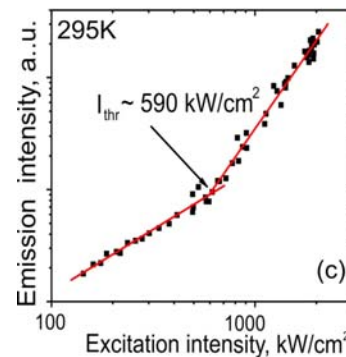
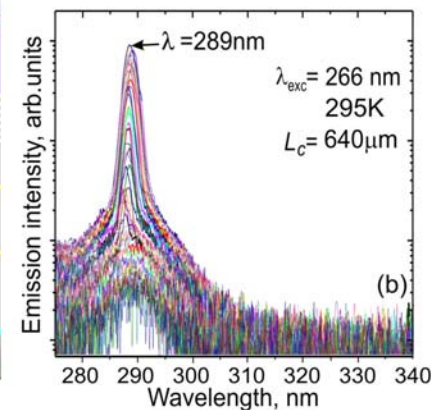
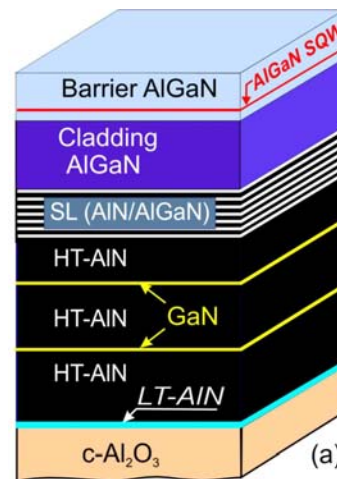
## Low-threshold 303 nm lasing in AlGaIn-based multiple-quantum well structures with an asymmetric waveguide grown by plasma-assisted molecular beam epitaxy on c-sapphire

V. N. Jmerik,<sup>1(a)</sup> A. M. Mizerov,<sup>1</sup> A. A. Sitnikova,<sup>1</sup> P. S. Kop'ev,<sup>1</sup> S. V. Ivanov,<sup>1</sup> E. V. Lutsenko,<sup>2</sup> N. P. Tarasuk,<sup>2</sup> N. V. Rzhetskii,<sup>2</sup> and G. P. Yablonskii<sup>2</sup>

<sup>1</sup>Ioffe Physical-Technical Institute, RAS, St. Petersburg 194021, Russia

<sup>2</sup>Stepanov Institute of Physics of NAS Belarus, Independence Ave. 68, Minsk 220072, Belarus

(Received 28 January 2010; accepted 2 March 2010; published online 8 April 2010)



Phys. Status Solidi A 210, No. 3, 439–450 (2013) / DOI 10.1002/pssa.201300006



Feature Article

Plasma-assisted molecular beam epitaxy of AlGaIn heterostructures for deep-ultraviolet optically pumped lasers

V. N. Jmerik<sup>1</sup>, E. V. Lutsenko<sup>2</sup>, and S. V. Ivanov<sup>1</sup>

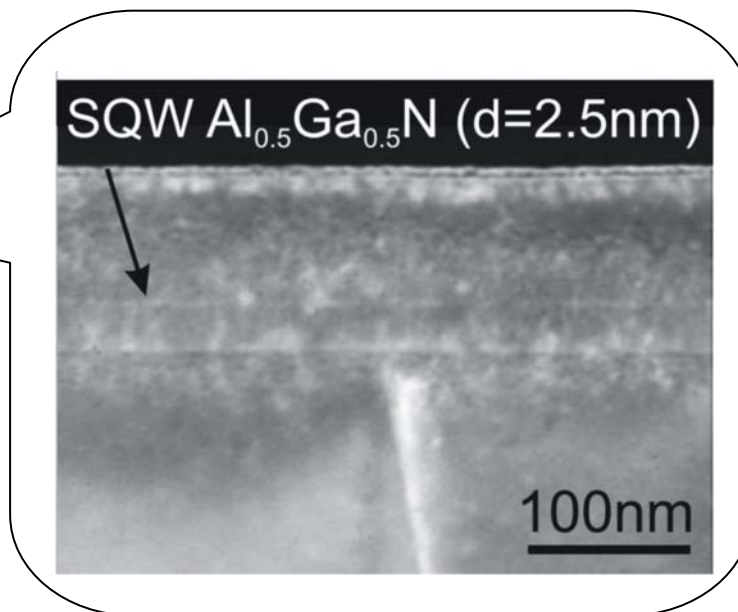
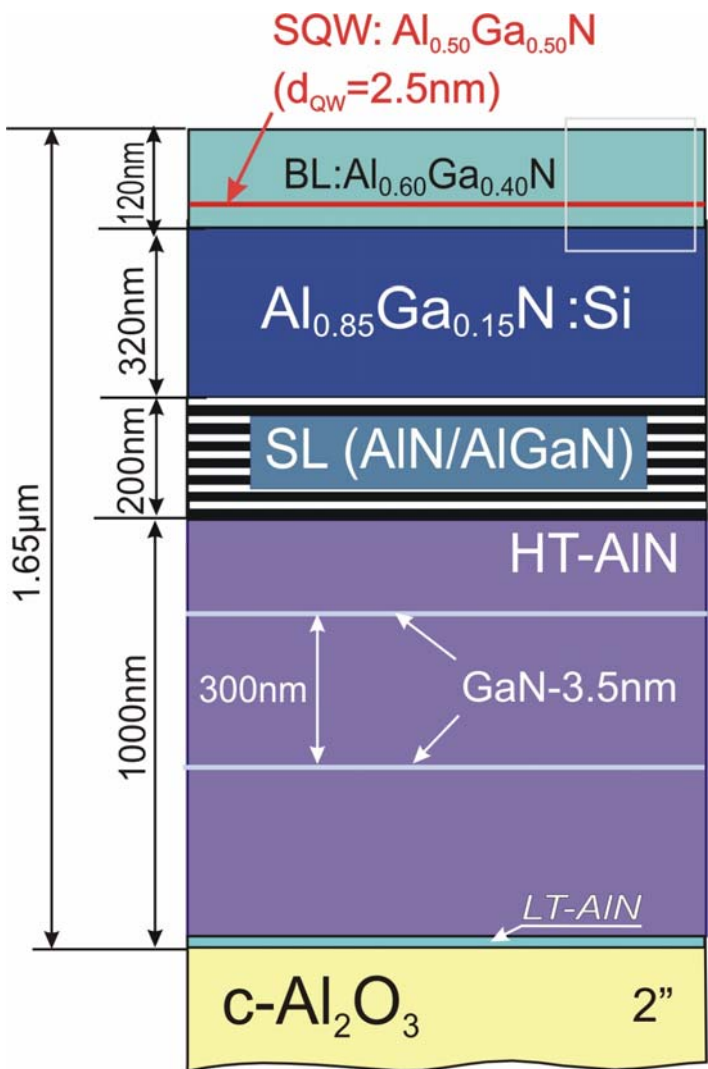
<sup>1</sup>Ioffe Physical-Technical Institute of RAS, Polytekhnicheskaya 26, St. Petersburg 194021, Russia

<sup>2</sup>Stepanov Institute of Physics of NAS Belarus, Independence Ave. 68, Minsk 220072, Belarus

Received 15 January 2013, revised 5 February 2013, accepted 6 February 2013  
Published online 4 March 2013



# Design and TEM image of AlGaN-based SQW structure optimized for sub-300nm UV-lasing



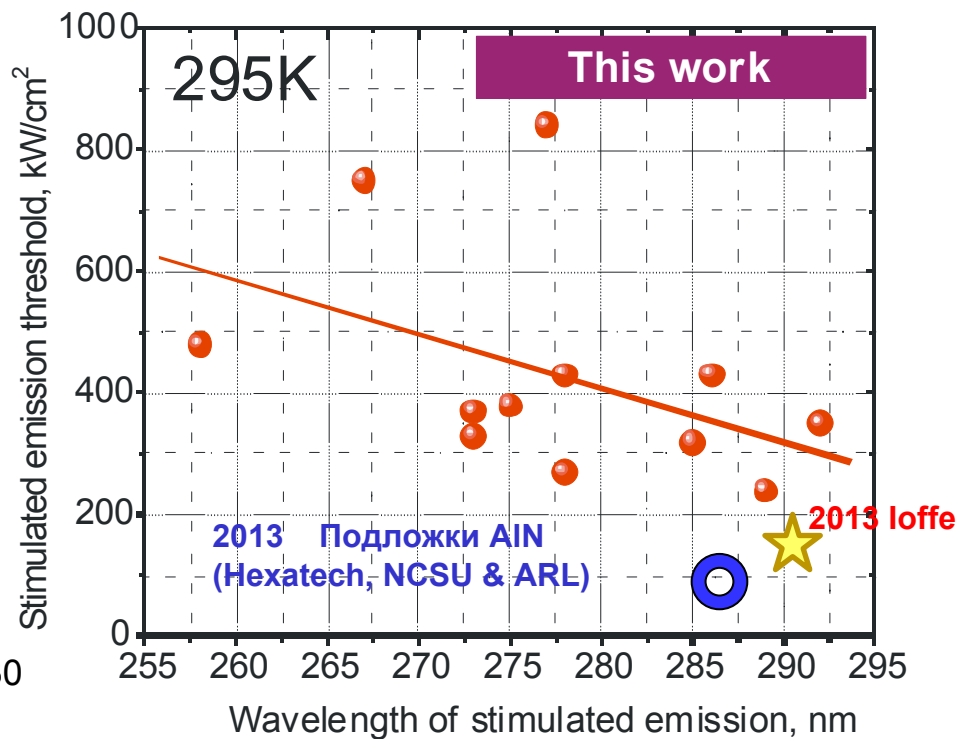
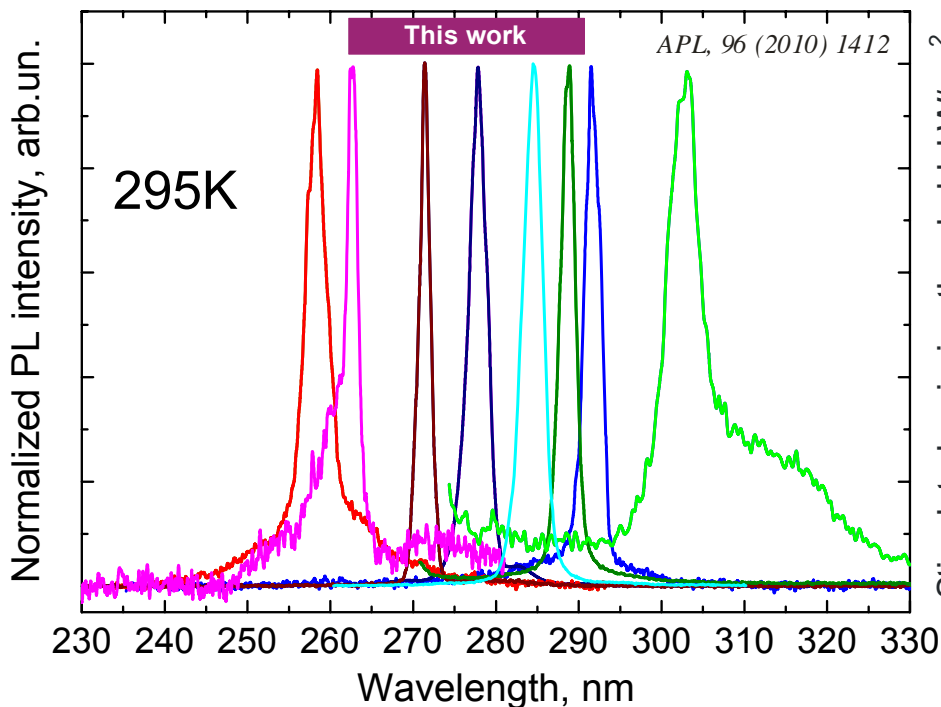
## Key factors

- Reduction of TDs density ( $10^8\text{-}10^9\text{cm}^{-2}$ ) by using (1-3)- $\mu\text{m}$  thick AlN buffer with incorporated optimized 3-nm-thick GaN layers and AlGaN/AlN SL, grown under the optimized conditions.
- Employing a SQW structure with optimum QW thickness  $<3\text{ nm}$  and slightly inhomogeneous morphology facilitating appearance of localization states.



# Stimulated emission in the sub-300nm range in AlGaN SQW SCH grown by PA MBE on c-Al<sub>2</sub>O<sub>3</sub>

Edge PL in cleaved-facets laser chips



Feature paper, Jmerik et al., phys. stat. sol. (a) 210, 439 (2013)

- Advanced AlGaN SQW and MQW structures grown by PA MBE on c-sapphire demonstrate optically-pumped stimulated emission within the 255-300 nm wavelength range with typical threshold power densities of 240-480 kW/cm<sup>2</sup> (295K) and TE polarization.
- The lowest SE threshold power density achieved at 289 nm was 150 kW/cm<sup>2</sup>.



# Outline

- Applications of UV-optoelectronics and state-of-the-art of AlGaN-based UV LED and laser structures obtained by both MOVPE and PA MBE
- PA MBE growth and surface morphology control of III-Nitrides
  - Al-rich growth of thick AlN/c-Al<sub>2</sub>O<sub>3</sub> buffer layers
  - Growth kinetics of AlGaN layers (2D-3D transition)
- Dislocation control and filtering in AlGaN/AlN/c-Al<sub>2</sub>O<sub>3</sub> heterostructures
- Sub-monolayer Digital Alloying growth of Al<sub>x</sub>Ga<sub>1-x</sub>N/Al<sub>y</sub>Ga<sub>1-y</sub>N QWs
- Strain engineering in AlGaN QW heterostructures to prevent TE/TM switching of photoluminescence polarization
- Low-threshold optically pumped QW laser structures in the 258-303 nm range
- LEDs and solar-blind p-i-n photodiodes
- Conclusions



# Electrical properties of as-grown PAMBE $\text{Al}_x\text{Ga}_{1-x}\text{N}:\text{Mg}$



**C-V (300K):** p-type  $p = 3 \times 10^{18} \text{ cm}^{-3}$

**Hall (250K):** p-type  $p = 1 \times 10^{18} \text{ cm}^{-3}$ ,  $\mu_H = 3 \text{ cm}^2/\text{Vs}$

**Seebeck (300K):** p-type



**C-V (300K):** compensated, although at the reverse bias above 5V p-type conductivity was observed

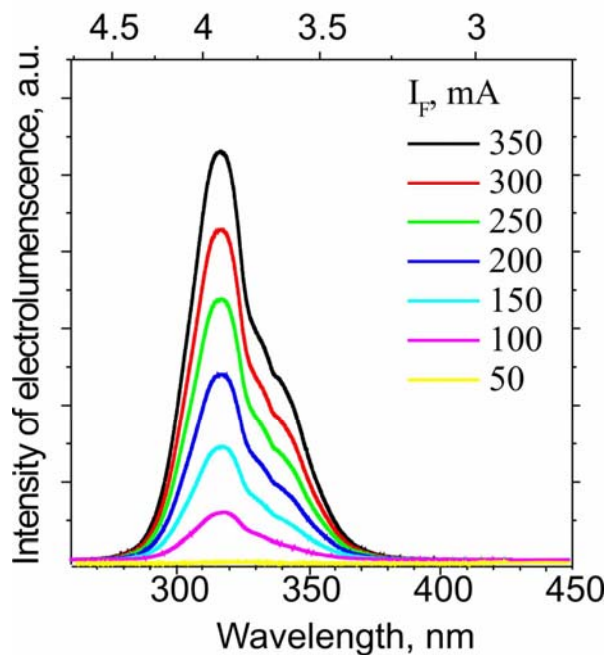
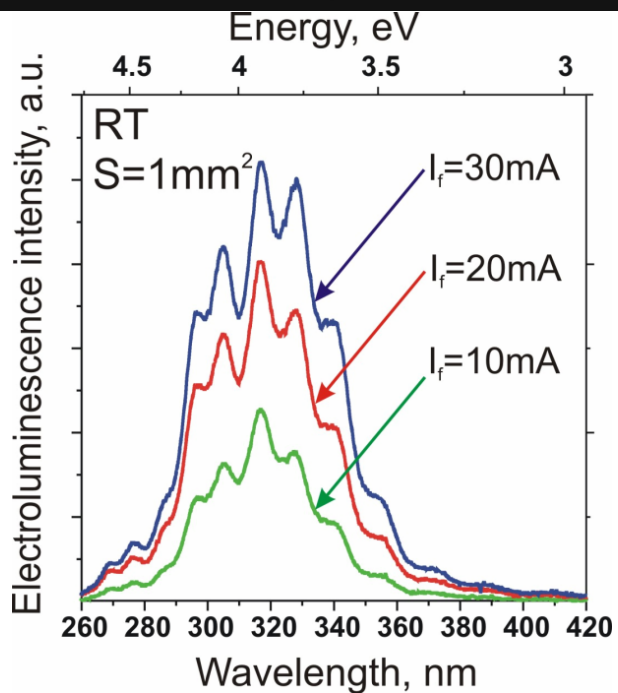
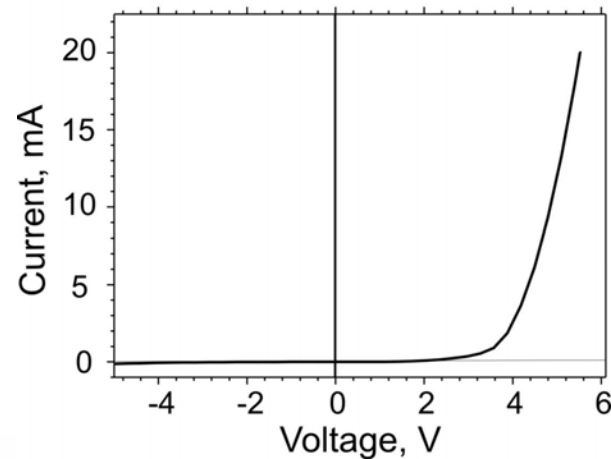
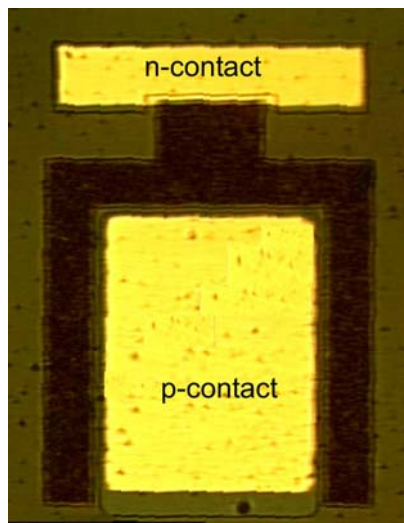
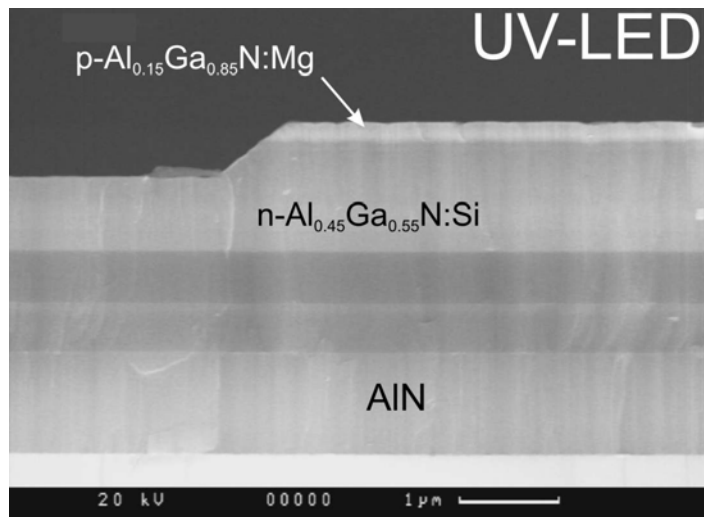
**Hall (250K):** p-type  $p = 4 \times 10^{17} \text{ cm}^{-3}$   $\mu_H = 1.4 \text{ cm}^2/\text{Vs}$

**Seebeck (300K):** p-type

**This is the first observation of p-conductivity by Hall effect in MBE-grown  $\text{Al}_x\text{Ga}_{1-x}\text{N}$  with  $x > 0.3$**



# Design and characteristics of UV LED

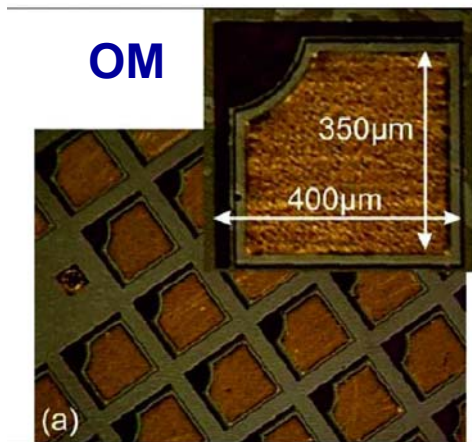
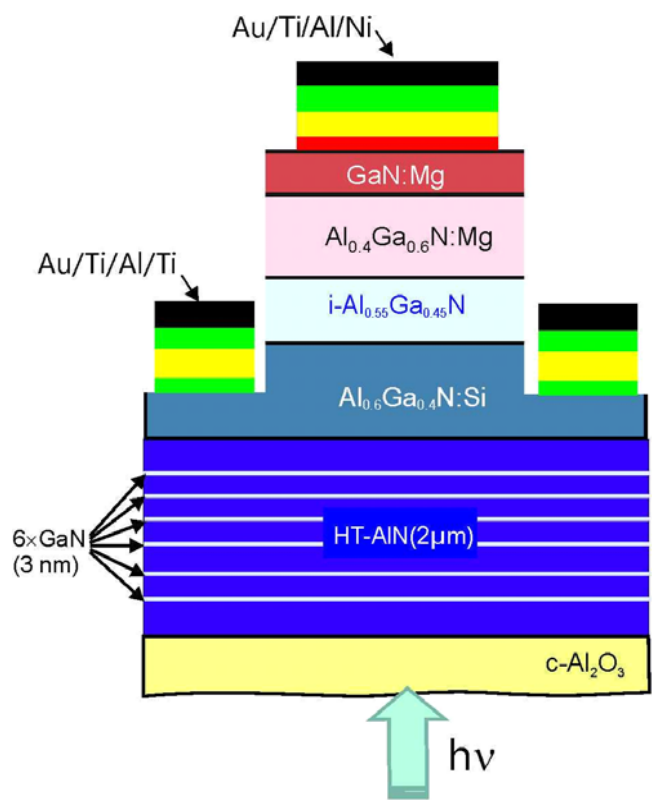


$\lambda = 300-350 \text{ nm}$

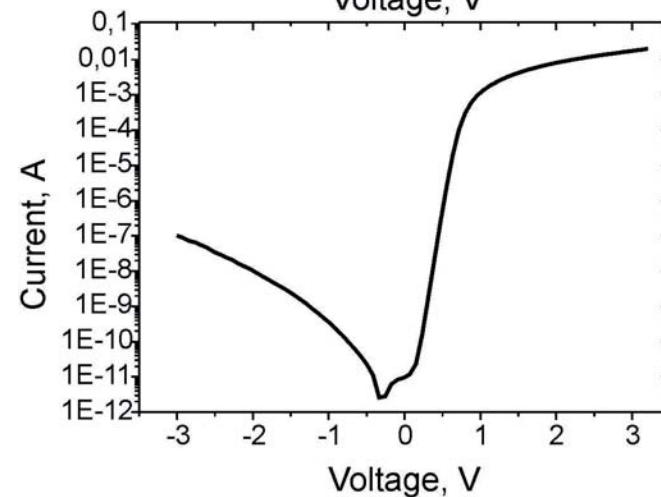
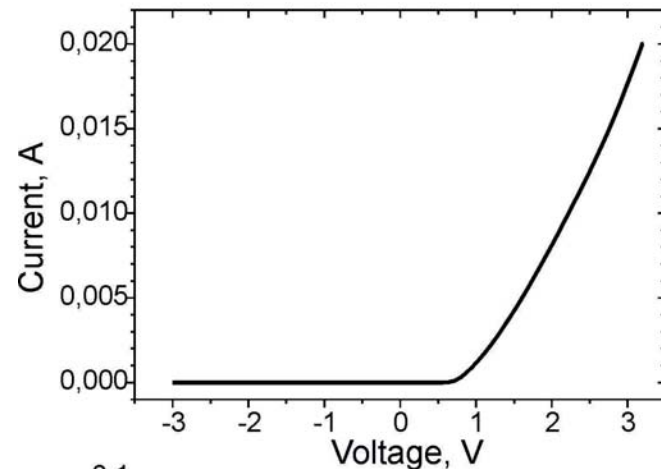
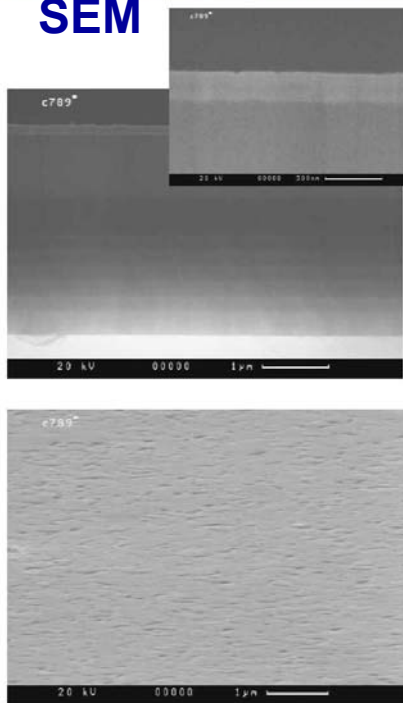
$P_{\text{out}} \sim 0.5 \text{ mW}$



# Development of solar-blind p-i-n UV-photodiode

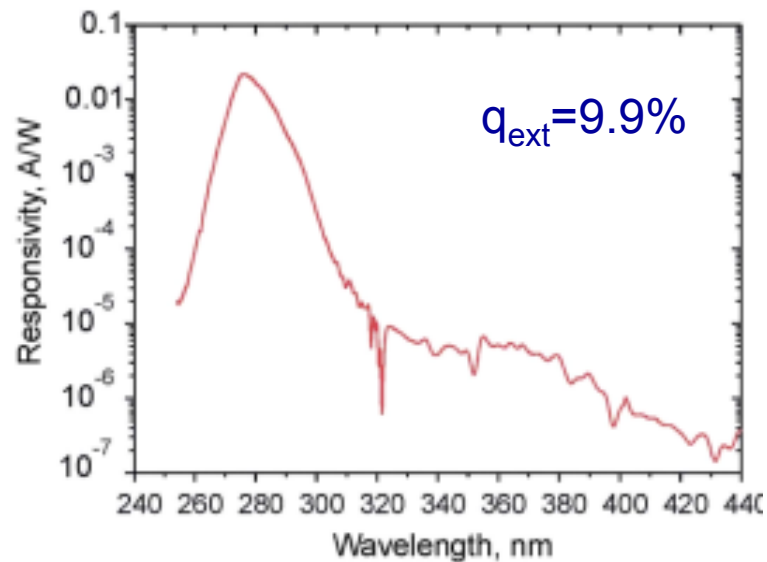
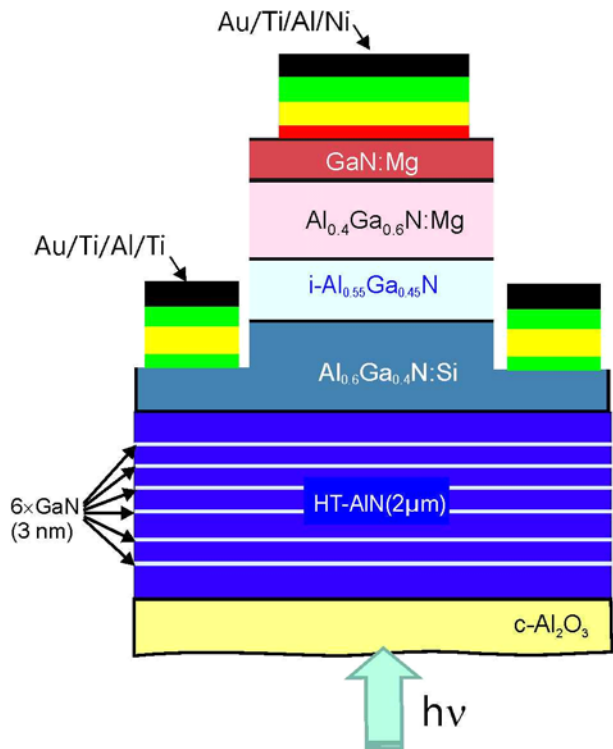


SEM

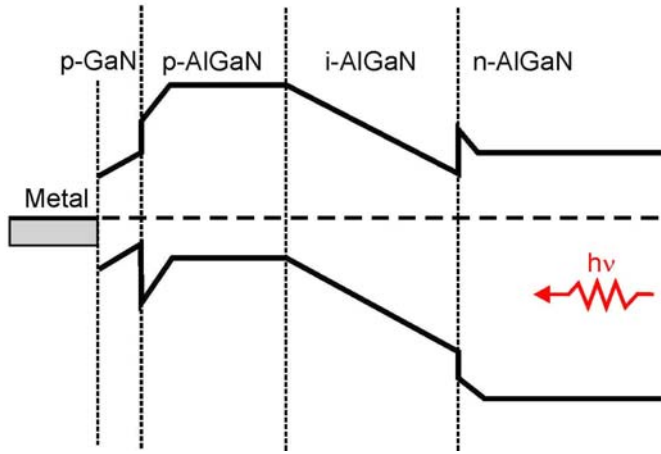




# Manufacturing both Schottky and p-i-n UV-photodiodes with the different level of Mg-doping



$$[Mg] = 6 \cdot 10^{18} - 2 \cdot 10^{19} \text{ cm}^{-3}$$





# Conclusions

- ✓ Advanced PA MBE growth technology of several-micron-thick AlN buffer layers with atomically-smooth and droplet-free surface morphology on c-Al<sub>2</sub>O<sub>3</sub> substrates has been developed, which employs pulsed supplied Al-flux under the quantitative control by laser reflectometry
- ✓ 2D-3D phase diagram of PA MBE of Al<sub>x</sub>Ga<sub>1-x</sub>N epilayers (x=0.2-1) on c-Al<sub>2</sub>O<sub>3</sub> substrates under the group III-rich conditions has been elucidated and substrate-temperature modulated epitaxy has been proposed to avoid Ga droplet formation.
- ✓ The most optimum combination of GaN interlayer parameters to maintain the 2D and cracking-free morphology of GaN/AlN buffer layers is as follows: mixed 2D-3D growth mode (streaky-dotty RHEED pattern), thickness of about 3nm, and interlayer spacing above 250 nm. TEM analysis has exhibited positive effect of the GaN insertions providing (i) inclination of both screw and edge TDs and (ii) blocking of vertical propagation of TDs due to bending in c-plane.
- ✓ Threading dislocations reduction and filtering using HT-MEE nucleation layer, optimized ultra-thin GaN interlayers in AlN buffer layer and strained AlN/AlGaN SL resulted in reduction of TD density in the active region grown atop down to 1.5×10<sup>8</sup> and 3×10<sup>9</sup> cm<sup>-2</sup> for screw and edge types, respectively. Lowest reported values for PA MBE.
- ✓ AlGaIn SQW and MQW structures have been fabricated by SMDA technique, which demonstrate RT PL within the wavelength range of 230-320 nm, PL decay time around 1 ns up to RT and intensity reduction just by 2.5 times from 77 to 300K.
- ✓ Pseudomorphic growth of Al<sub>x</sub>Ga<sub>1-x</sub>N/AlN (x>0.5) heterostructures has been implemented on c-Al<sub>2</sub>O<sub>3</sub> substrates to suppress transition from TE to TM polarization of photoluminescence as the wavelength decreases.
- ✓ Advanced AlGaIn SQW and MQW structures grown by PA MBE on c-sapphire demonstrate optically-pumped stimulated emission within the 255-300 nm wavelength range with typical threshold power densities of 240-480 kW/cm<sup>2</sup> (295K) and TE polarization. The lowest laser threshold power density achieved at 289 nm was 150 kW/cm<sup>2</sup>.
- ✓ Mid-UV LEDs and solar-blind photodiodes have been demonstrated.

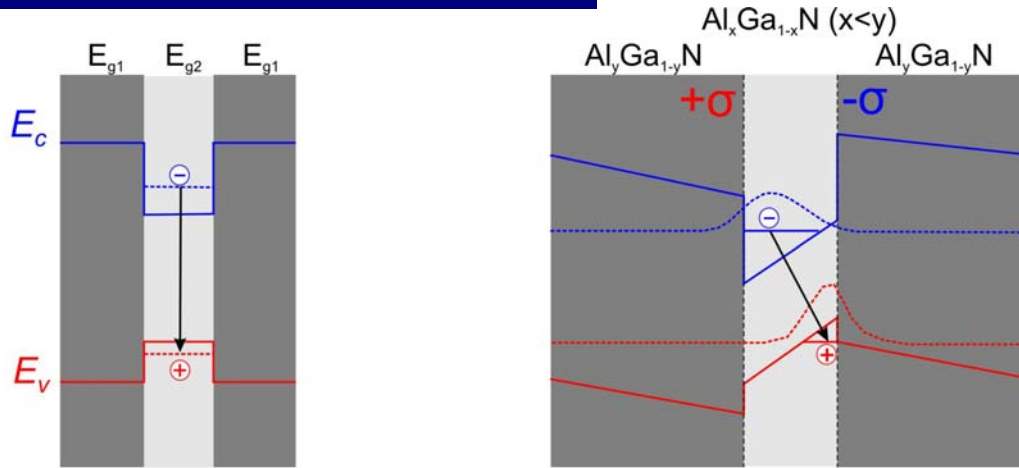


**Thank you for the attention**

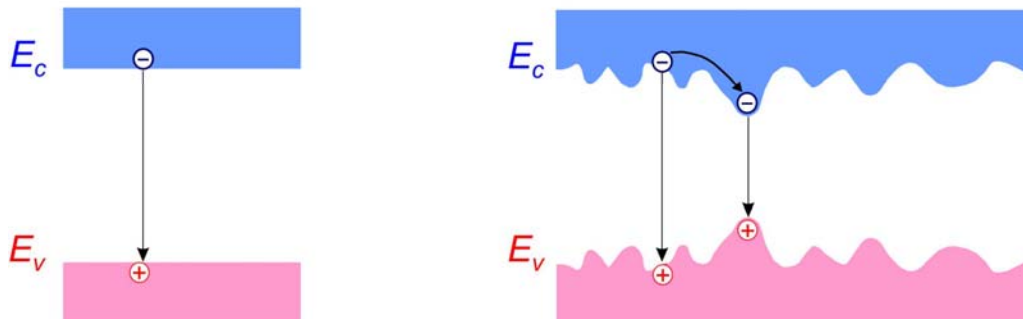


# Main effects determining the light emission mechanisms in AlGaIn-based (0001) QWs

## Quantum –confined Stark effect



## Localized states due to potential fluctuations (compositional inhomogeneities)

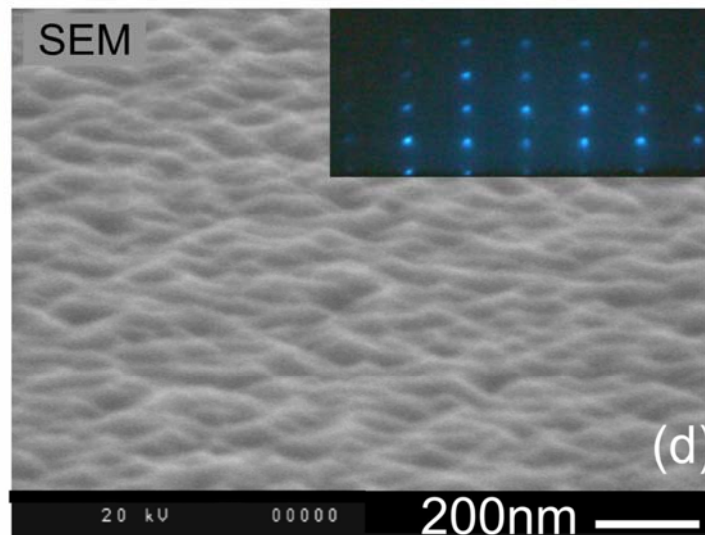
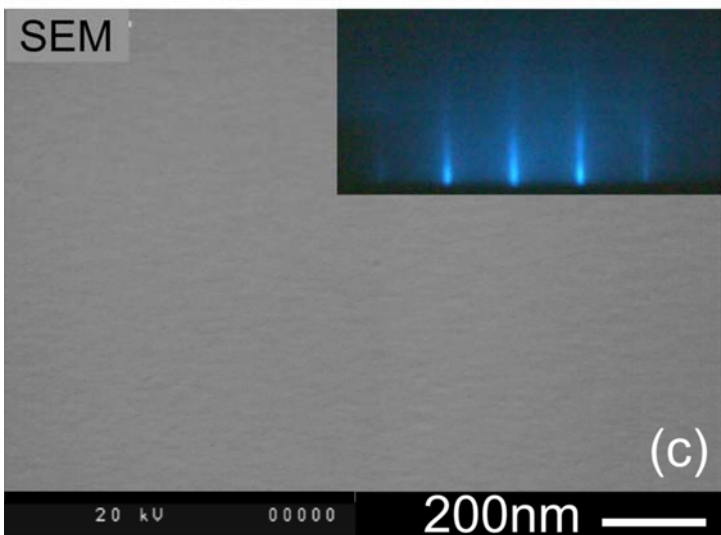
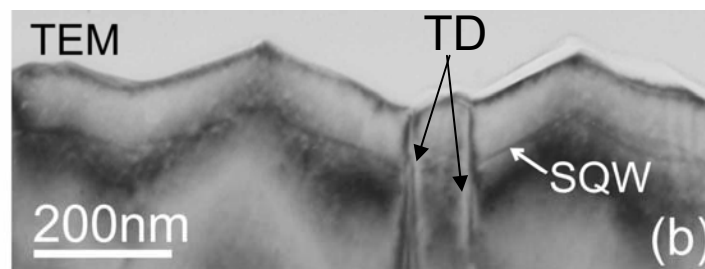
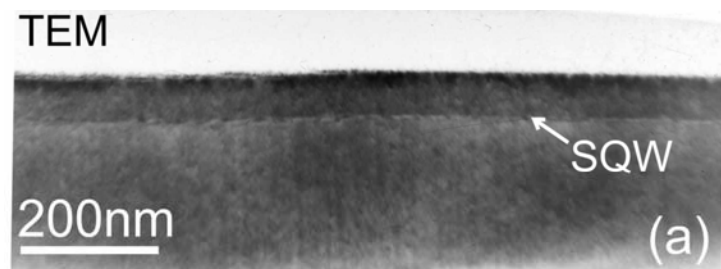


### Varied technological parameters:

- Al-composition in  
Barrier layers:  $y=0.4-0.6$   
QWs:  $x=0.3-0.5$
- Thickness of QW: 2.5-6nm
- Morphology: plane vs corrugated
- Growth temperature: 670-730°C



# 6-nm-thick $\text{Al}_{0.3}\text{Ga}_{0.7}\text{N}/\text{Al}_{0.4}\text{Ga}_{0.6}\text{N}$ SQW structures with plane and corrugated morphology grown by SMDA



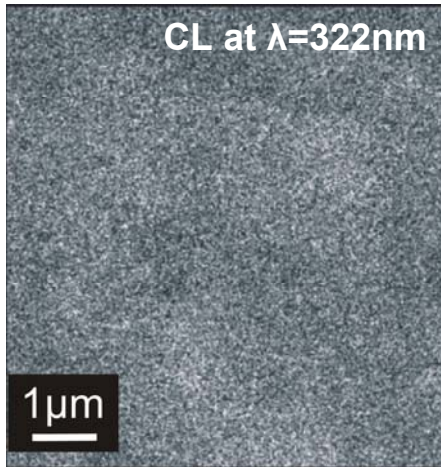
2D AlN buffer growth mode

3D AlN buffer growth mode

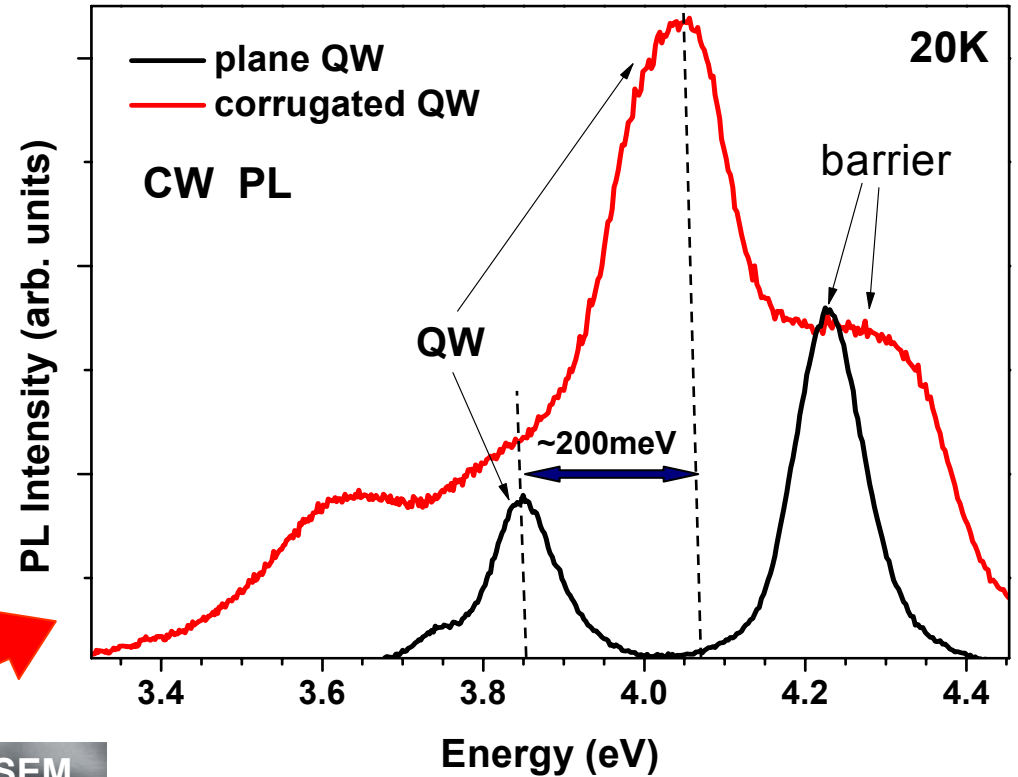
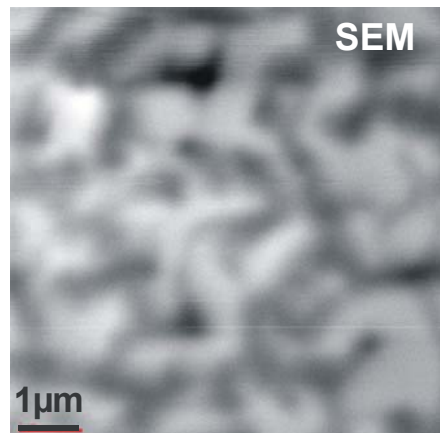
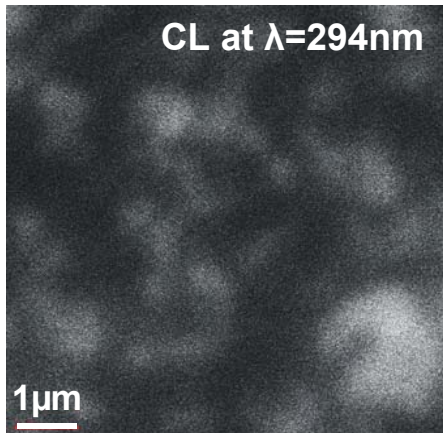
For both structures  $N_D \sim 10^{10} \text{ cm}^{-2}$

# CL images and cw-PL spectra of the AlGaN SQW structures with different morphologies

Plane QW morphology



Corrugated QW morphology



- 4 times stronger PL emission in the corrugated QW at 20K
- 200 meV red shift of PL peak in planar QW

**Suppressed QCSE?**

*Shevchenko et al., Semiconductors, 46, 8, 1022 (2012)*

*Peking University, May 15, 2014*